JACC: CARDIOONCOLOGY VOL. 2, NO. 2, 2020

STATE-OF-THE-ART REVIEW

Magnetic Resonance Imaging to Detect Cardiovascular Effects of Cancer Therapy

JACC CardioOncology State-of-the-Art Review

Iwan Harries, MBBCH,[a] Kate Liang, MBBCH,[a] Matthew Williams, MBCHB,[a] Bostjan Berlot, MD,[a,b] Giovanni Biglino, PHD,[a,c] Patrizio Lancellotti, MD, PHD,[d,e] Juan Carlos Plana, MD,[f] Chiara Bucciarelli-Ducci, MD, PHD[a]

ABSTRACT

This paper aims to empower and inform cardio-oncologists by providing a practical guide to the clinical application of cardiac magnetic resonance (CMR) in the rapidly evolving field of cardio-oncology. Specifically, we describe how CMR can be used to assess the cardiovascular effects of cancer therapy. The CMR literature, relevant societal guidelines, indication-specific imaging protocols, and methods to overcome some of the challenges encountered in performing and accessing CMR are reviewed. (J Am Coll Cardiol CardioOnc 2020;2:270–92) © 2020 The Authors. Published by Elsevier on behalf of the American College of Cardiology Foundation. This is an open access article under the CC BY-NC-ND license (http://creativecommons.org/licenses/by-nc-nd/4.0/).

Advances in treatment and supportive care have led to improved survival for patients with cancer. However, cancer therapy confers cardiovascular risk, and patients with established cardiovascular disease receiving cancer treatment are particularly susceptible to cardiovascular complications (1). Consequently, collaboration between cardiologists and oncologists and the emergence of dedicated specialists in the emerging field of cardio-oncology are becoming increasingly important. Cardiac magnetic resonance (CMR) is a multiparametric imaging modality that is changing clinical practice, and has a wide variety of applications and enormous potential in cardio-oncology. This article aims to empower and inform cardio-oncologists by providing a practical guide to the clinical applications of CMR in patients during and after cancer therapy. The CMR literature, relevant guidelines, indication-specific imaging protocols, and methods to overcome some of the limitations and challenges encountered in CMR are also discussed. We describe each CMR imaging sequence, its potential application, and guideline-directed indications for CMR. We also refer the reader to the recently published appropriate use criteria (2), the Society for Cardiovascular Magnetic Resonance guidelines for standardized CMR protocols (3), CMR

From the [a]Bristol Heart Institute, Bristol National Institute of Health Research (NIHR) Biomedical Research Centre, University Hospitals Bristol NHS Trust and University of Bristol. Bristol, United Kingdom; [b]Department of Cardiology, University Medical Centre Ljubljana, Slovenia; [c]National Heart and Lung Institute, Imperial College London, London, United Kingdom; [d]University of Liège Hospital, GIGA Cardiovascular Sciences, Departments of Cardiology, Heart Valve Clinic, CHU Sart Tilman, Liège, Belgium; [e]Gruppo Villa Maria Care and Research, Anthea Hospital, Bari, Italy; and the [f]Texas Heart Institute at Baylor St. Luke's Medical Center, Baylor College of Medicine, Houston, Texas, USA. Dr. Bucciarelli-Ducci is in part supported by the National Institutes of HealthR Biomedical Research Centre at University Hospitals Bristol NHS Foundation Trust and the University of Bristol. The views expressed in this publication are those of the author(s) and not necessarily those of the NHS, the National Institute for Health Research, or the Department of Health and Social Care. Dr. Bucciarelli-Ducci is the CEO of the Society for Cardiovascular Magnetic Resonance (part-time). All other authors have reported that they have no relationships relevant to the contents of this paper to disclose.
The authors attest they are in compliance with human studies committees and animal welfare regulations of the authors' institutions and Food and Drug Administration guidelines, including patient consent where appropriate. For more information, visit the *JACC: CardioOncology* author instructions page.

Manuscript received December 6, 2019; revised manuscript received April 12, 2020, accepted April 15, 2020.

ISSN 2666-0873 https://doi.org/10.1016/j.jaccao.2020.04.011

HIGHLIGHTS

- Cancer therapy improves cancer survival but can result in a variety of cardiovascular toxicities.
- Cardiovascular magnetic resonance is an extremely versatile and useful tool to assess cardiovascular toxicities of cancer therapy.
- Technological improvement, collaboration, research, and education are essential to the evolving use of cardiovascular magnetic resonance in cardio-oncology.

image interpretation and post-processing (4), and principles of CMR reporting (5) for additional useful references.

CMR IMAGING SEQUENCES AND REFERRAL

CMR uses different imaging sequences to provide comprehensive information about the cardiovascular system that is tailored to the clinical question posed. The CMR protocol is typically chosen based on the information provided by the referring physician. It is therefore important that all relevant background information is included, and the clinical question clearly formulated in the study request (**Central Illustration**). Each sequence provides specific anatomical, tissue characteristics, functional, flow, or perfusion data (**Table 1**). A combination of sequences is selected to create the CMR protocol (**Figure 1**).

ANATOMY: DARK BLOOD (T1- AND T2-WEIGHTED) AND WHITE BLOOD IMAGING. CMR protocols typically begin with cross-sectional axial and/or coronal images that describe the anatomy of the thorax and upper abdomen (**Figure 2**). Major incidental extracardiac findings were reported to occur in 12% of CMR studies that were performed for any indication in a recent meta-analysis (6). These findings may prompt additional investigations, and can contribute to contextualizing the underlying cardiovascular diagnosis.

Anatomical sequences can provide both direct anatomical information, for example, pericardial thickening following radiation (**Figure 3A**), and indirect information relating to the hemodynamic consequences of underlying disease, for example, pleural effusions (**Figure 3B**). Incidental findings, such as primary or secondary malignancies, may also be encountered (**Figures 3C and 3D**). Anatomical sequences also help to describe tissue properties; for example, fluid appears bright on T2-weighted images.

CARDIAC FUNCTION, VENTRICULAR VOLUMES, AND MASS: STEADY-STATE FREE PRECESSION CINE SEQUENCES. CMR is the reference standard for the assessment of ventricular volumes and ejection fraction with high levels of accuracy and reproducibility, both in health and disease in the left (7,8) and right ventricle (9). Steady-state free precession (SSFP) cine sequences provide high resolution, time-resolved images that allow excellent discrimination of the endocardial and epicardial borders, which are subsequently contoured to provide 3-dimensional (3D) estimations of ventricular volumes, function, and mass. The left ventricle is conventionally assessed in 3 long-axis planes and a stack of contiguous short-axis "slices" from the left ventricular base in the atrioventricular plane to the apex (**Figure 4**). The long-axis planes are similar to those obtained by echocardiography: 4-chamber (4C), 3-chamber (3C) and 2-chamber (2C) (**Figure 4**). The right ventricle can also be evaluated in the same short-axis stack (**Figure 4**) or alternatively with an axial stack with similarly high levels of interobserver and intraobserver reliability reported for each method (10).

Endocardial borders are contoured at end-diastole and end-systole in each of the short-axis (or axial) slices to provide 3D volumes that do not rely on the geometric assumptions of 2D methods. However, volume estimation by CMR relies on different geometric assumptions, and although the papillary muscles are part of the myocardium, in clinical practice, they are often included as part of the blood pool and thus contribute to ventricular volume (11). Regional wall motion can be assessed either subjectively or objectively (using wall-thickening or myocardial strain) and is conventionally reported by dividing the left ventricle into 17 equally weighted segments, as recommended by the American Heart Association writing group on myocardial segmentation and registration for cardiac imaging (12).

Measurement of left ventricular volumes, ejection fraction, and mass by CMR are highly accurate and have been shown to be more reproducible (coefficient of variation for left ventricular ejection fraction [LVEF] in normal subjects is 2.4%) than left ventricular volumes and mass by echocardiography (coefficient of variation for LVEF in normal subjects up to 8.6%) or radionuclide ventriculography (7,8). Consequently, CMR has been used in some cardio-oncology research trials for precise serial evaluation of cardiac structure and function (13,14).

ABBREVIATIONS AND ACRONYMS

CMR = cardiac magnetic resonance

ECV = extracellular volume fraction

EGE = early gadolinium enhancement

ICI = immune checkpoint inhibitors

LGE = late gadolinium enhancement

LVEF = left ventricular ejection fraction

MACE = major adverse cardiac event

SSFP = balanced steady state free precession

CENTRAL ILLUSTRATION **Typical Cardiovascular Effects of Classes of Cancer Therapy With Suggested Cardiovascular Magnetic Resonance Imaging Protocols**

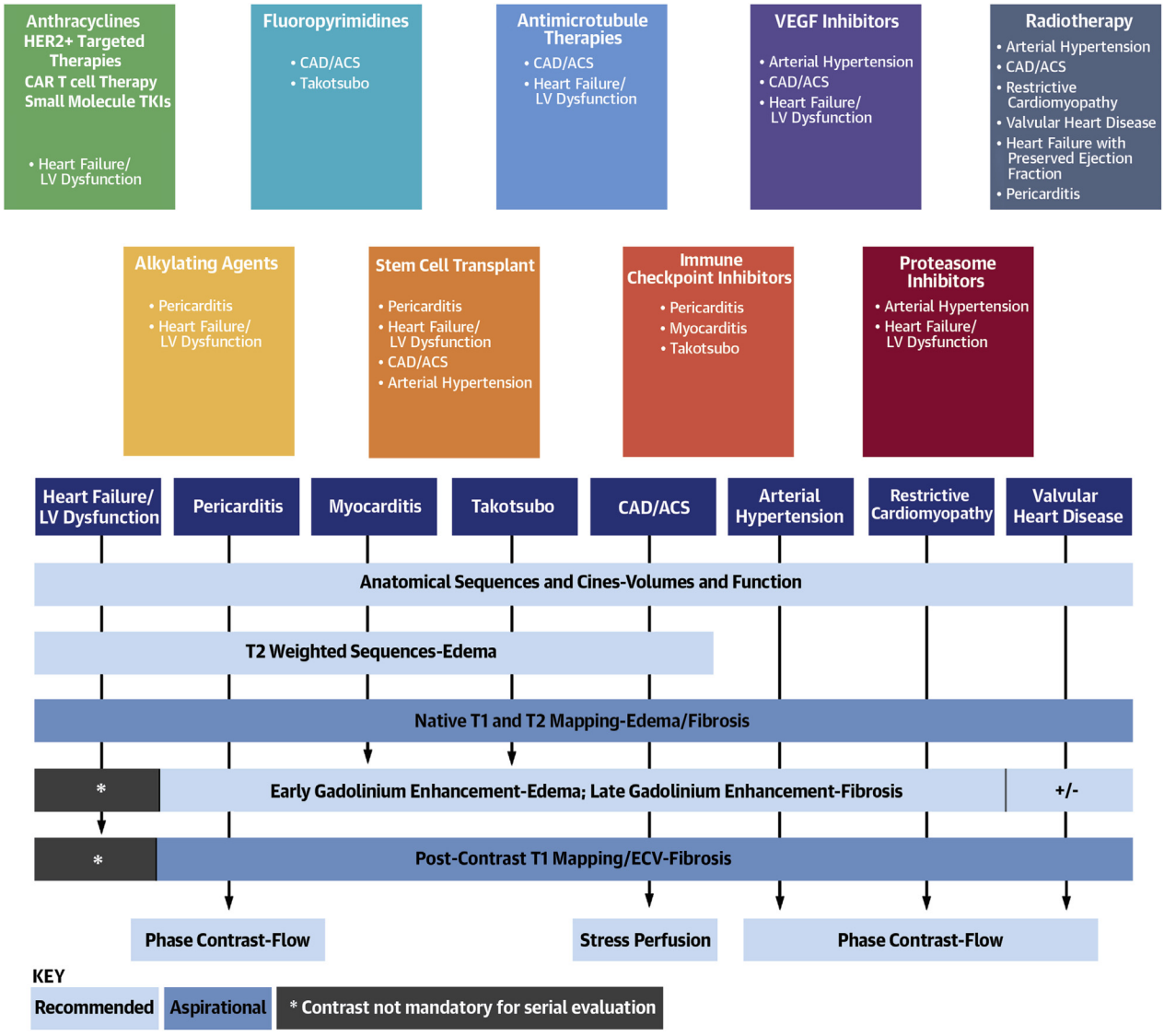

Harries, I. et al. J Am Coll Cardiol CardioOnc. 2020;2(2):270–92.

The typical cardiovascular effects of various classes of cancer therapy, together with suggested cardiovascular magnetic resonance (CMR) imaging protocols and key metrics provided by each sequence. "Recommended" and "aspirational" CMR imaging sequences to characterize the respective pathologies are suggested. For specific data on the timing and incidence of toxicity, please see relevant literature (1,66,72,80,81,91,110-113). *Contrast administration may not necessarily be required for serial evaluation of left ventricular function. ACS = acute coronary syndrome; CAD = coronary artery disease; ECV = extracellular volume fraction; HER2+ = human epidermal growth factor receptor; LV = left ventricular; TKI = tyrosine kinase inhibitor; VEGF = vascular endothelial growth factor.

The left ventricular myocardium is an architecturally complex structure that deforms in longitudinal (along the long axis, apex to base), circumferential (along the circular axis) and radial (towards the center of the ventricle) planes. Methods to quantify myocardial deformation, or "strain," rely on the principle of tracking distinctive features over successive images and several CMR sequences have been developed for this purpose. These include tagging, displacement encoding with simulated echoes, phase

TABLE 1 Key Features of Common CMR Imaging Sequences and Relevant Uses

Sequence	Features	Relevant Clinical Uses
Anatomy and localizers	Rapidly acquired Dark blood (Figures 2A to 2D) which can be: T1-weighted (better anatomic definition)* or T2-weighted (better tissue characterization)† White blood (Figures 2E to 2H)	Assessment of extracardiac structures (Figure 3) Localizers used to plan cardiac imaging planes
Cines	Use SSFP (a type of gradient echo pulse sequence) to produce a short movie or "cine" of the heart moving (Figures 4, 5, and 10A to 10B)	Assessment of ventricular volumes, systolic function, and dynamic motion of thrombus (e.g., Figure 6A)
Edema	T2-weighted imaging (e.g., T2 STIR) Must be acquired before contrast administration	Qualitative assessment of myocardial edema, as in ICI-associated myocarditis or Takotsubo cardiomyopathy
Native T1 mapping	Popular methods include MOLLI and SASHA Quantifies native (noncontrast) T1 relaxation time	Quantitative assessment of myocardial fibrosis (Figure 8) Quantitative assessment of myocardial edema (both display prolonged T1 relaxation time)
Native T2 mapping	Typically uses SSFP sequence preceded by T2 preparation module. Quantifies native (noncontrast) T2 relaxation time	Quantitative assessment of myocardial edema (prolonged T2 relaxation time)
Perfusion	T1-weighted saturation recovery gradient echo pulse sequence Gadolinium contrast administered and imaged over >40 heart beats	Assessment of vascularity, e.g., an intracardiac mass
Stress perfusion	As above but performed under conditions of pharmacologic stress, e.g., adenosine or dobutamine	Assessment of coronary artery disease; perfusion defects evident in ischemic myocardium (Figure 10A)
EGE	Inversion recovery gradient echo sequence Performed 1-3 min after contrast administration	Assessment of intracardiac thrombus, which is avascular and therefore appears black (Figures 6B and 6D)
LGE	Inversion recovery gradient echo sequence Performed >10 min after contrast administration (delay may need to be adjusted according to dose, cardiac output) Normal myocardium is "nulled" to appear black	Assessment of focal fibrosis, e.g., in myocardial infarction, which appears white (Figures 7A to 7C and 10B)
Post-contrast T1 mapping	Popular methods include MOLLI and SASHA Quantifies post-contrast T1 relaxation time	Allows calculation of ECV using hematocrit, native and post-contrast T1 relaxation times of myocardium, and blood pool. ECV is elevated in conditions associated with expansion of the myocardial interstitium (e.g., amyloid)
Phase contrast	Uses bipolar gradients Typically acquired in a plane perpendicular to blood flow	Assessment of valvular heart disease, including velocity and direction of blood flow (Figure 11C) Allows estimation of severity of stenotic and regurgitant lesions.

*T2-weighted relies on transverse relaxation: fluid = high signal intensity (white), muscle = intermediate signal intensity (grey), fat = high signal intensity (white). †T1-weighted relies on longitudinal relaxation: fluid = low signal intensity (black); muscle = intermediate signal intensity (grey); fat = high signal intensity (white).

CMR = cardiovascular magnetic resonance; ECV = extracellular volume; EGE = early gadolinium enhancement; ICI = immune checkpoint inhibitor; LGE = late gadolinium enhancement; MOLLI = modified look-locker; SASHA = saturation recovery single shot acquisition; SSFP = steady-state free precession; STIR = short Tau inversion recovery

velocity mapping, strain-encoded imaging and latterly, feature tracking. An advantage of the feature-tracking strain is that it can be calculated from standard cine sequences (Figure 5), whereas the other methods require dedicated sequences to be acquired. There is emerging evidence of a significant incremental prognostic role for CMR strain when added to LVEF and late gadolinium enhancement (LGE) techniques in both ischemic and dilated cardiomyopathies (15). A systematic review of echocardiography-derived myocardial deformation studies confirmed the value of these parameters for the early detection of myocardial changes and prediction of cardiotoxicity (16). The utility of strain-guided echocardiography monitoring of patients receiving cardiotoxic cancer therapy in comparison to standard care is currently being evaluated by the SUCCOUR (Strain Surveillance of Chemotherapy for Improving Cardiovascular Outcomes) randomized controlled trial (17). Although the CMR-derived strain literature is in its infancy, initial reports confirm detectible temporal changes in circumferential (18-20) and longitudinal (20) strain in patients receiving cardiotoxic chemotherapy. The sensitivity of strain in comparison to LVEF-based techniques suggests that it has the potential to play an important role in the early detection of cardiotoxicity, although large-scale confirmatory evidence is currently lacking. In comparison to speckle-tracking echocardiography, CMR-based feature tracking shows good agreement and appears to have comparable levels of reproducibility (21). However, strain has limitations. The range of vendors (hardware and software), acquisition techniques, and post-processing algorithms means that normal reference ranges are difficult to establish. Furthermore, interobserver and intraobserver variability as well as interstudy reproducibility continue to present barriers to widespread clinical use.

EDEMA/INFLAMMATION: T2-WEIGHTED IMAGING AND NATIVE T2 MAPPING. CMR is the reference standard imaging technique to detect myocardial

FIGURE 1 Typical Composition of a CMR Imaging Protocol

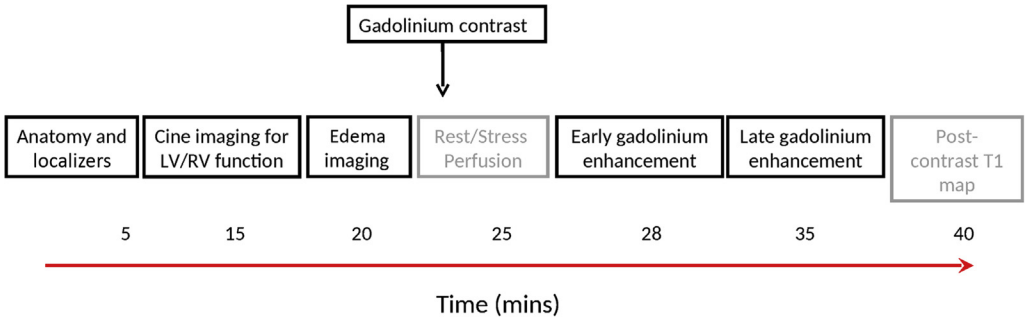

CMR protocols are composed of different imaging sequences and tailored to the clinical question posed. Example additional imaging sequences are represented in **grey**. Native (non-contrast) and contrast-enhanced sequences occur before and after gadolinium administration, respectively. CMR = cardiovascular magnetic resonance; LV = left ventricle; RV = right ventricle.

hyperemia and edema using both T2- and T1-weighted imaging sequences (22,23). Regions of edema/inflammation exhibit higher signal intensity/enhancement on these sequences. The T2-weighted short-tau inversion recovery (T2 STIR) sequence is commonly used, although T2 mapping and early gadolinium enhancement (T1-weighted) are also used. Some of these sequences are assessed qualitatively (e.g., T2 STIR) by adjudicating signal intensity in different myocardial segments, or by obtaining a ratio of signal intensity between the myocardium and skeletal muscle; whereas others are assessed quantitatively by drawing "regions of interest" that provide a T2 mapping value in milliseconds (e.g., T2 mapping). Native myocardial T2 mapping is reported to be the most reproducible method in the setting of edema associated with myocardial infarction (24) and the utility of parametric mapping methods was recognized by the updated Lake Louise criteria for the evaluation of nonischemic myocardial inflammation

FIGURE 2 Example Anatomical CMR Sequences

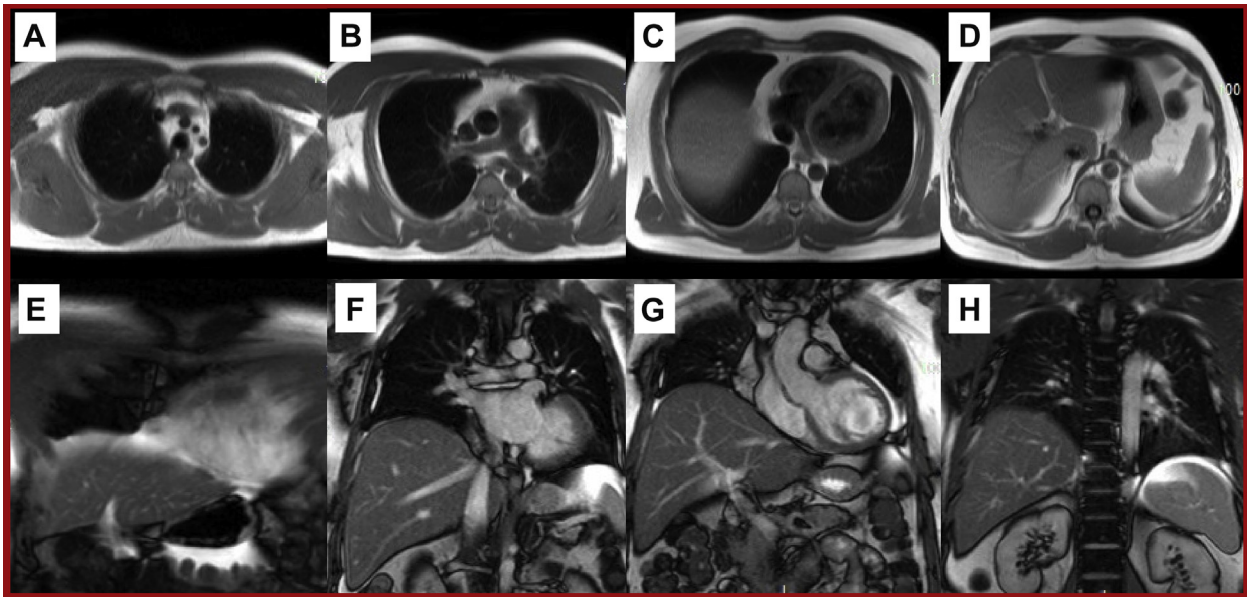

Sequential axial black blood **(A to D)** and coronal white blood **(E to H)** images through the thorax and upper abdomen. Abbreviation as in Figure 1.

FIGURE 3 **Abnormalities Detected on Anatomical Sequences**

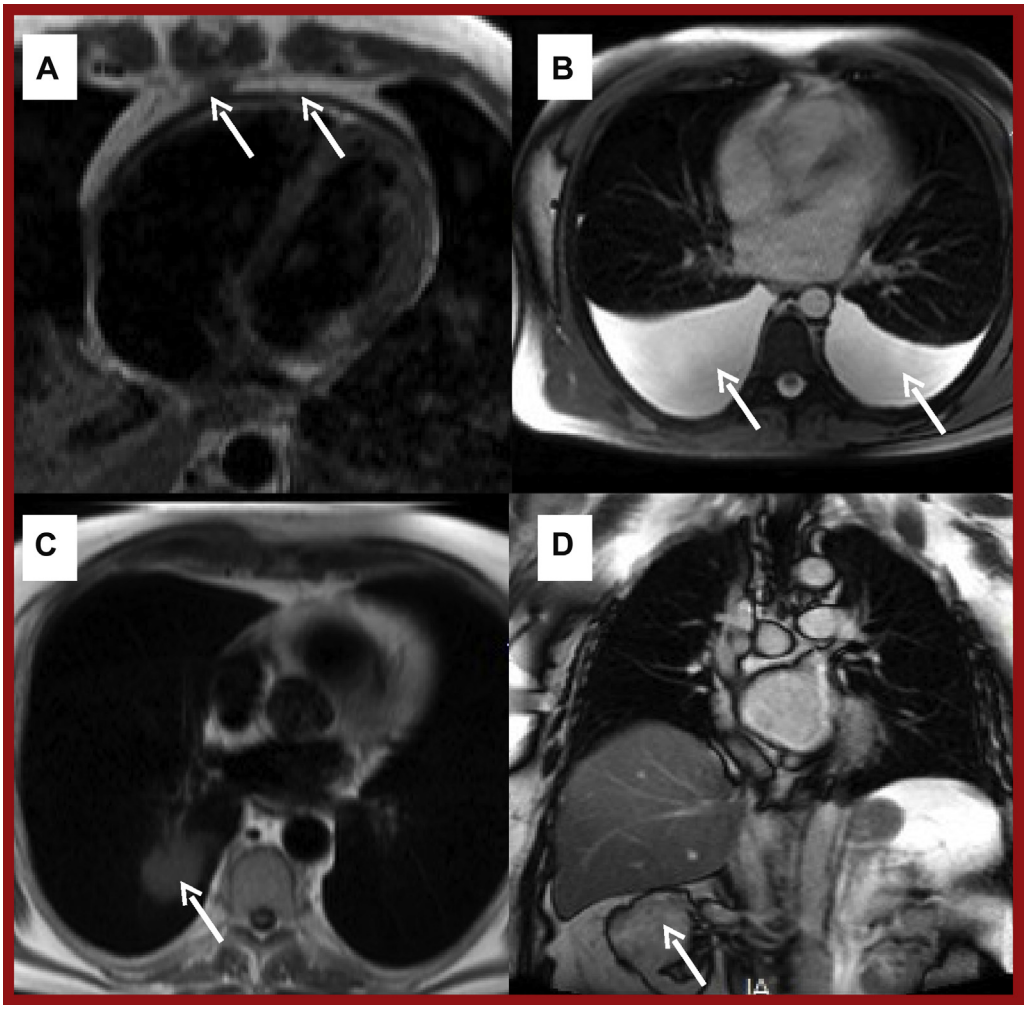

(A) T1-weighted black blood turbo spin echo showing diffuse pericardial thickening **(arrows). (B)** White blood T2-weighted axial sequence showing bilateral pleural effusions **(arrows)** due to constrictive pericarditis (same patient A). **(C)** Incidental right lung tumor **(arrow). (D)** Incidental right renal tumor **(arrow).**

(25). Recent animal (26) and human (27) studies have reported the potential utility of native myocardial T2 mapping as a biosignature of early cancer therapy-associated toxicity.

TISSUE PERFUSION: STRESS PERFUSION SEQUENCES. Perfusion sequences performed in conjunction with pharmacologic stress are designed to determine if there is inducible myocardial hypoperfusion due to epicardial coronary stenosis. Typically, a stack of 3 short-axis slices (base, mid, and apex) are acquired. Myocardium supplied by a stenotic vessel appears dark and "hypoperfused" in comparison to well-perfused myocardium, which appears bright.

DETECTION OF INTRACARDIAC THROMBUS AND MYOCARDIAL HYPEREMIA/EDEMA: T1-WEIGHTED EARLY GADOLINIUM ENHANCEMENT IMAGING. Following the administration of a gadolinium-based contrast agent, the contrast redistributes from the blood pool into the myocardium. Between 2 and 5 min after contrast administration, this results in the blood pool and myocardium appearing hyperintense in early gadolinium enhancement (EGE) sequences. Therefore, these sequences can be useful in distinguishing between intracardiac thrombus, the most common cardiac pseudotumor (28), and true cardiac tumors by virtue of the fact that thrombi are inherently avascular, do not uptake gadolinium, and

FIGURE 4 Steady-State Free Precession "Cine" Images of the Left Ventricle

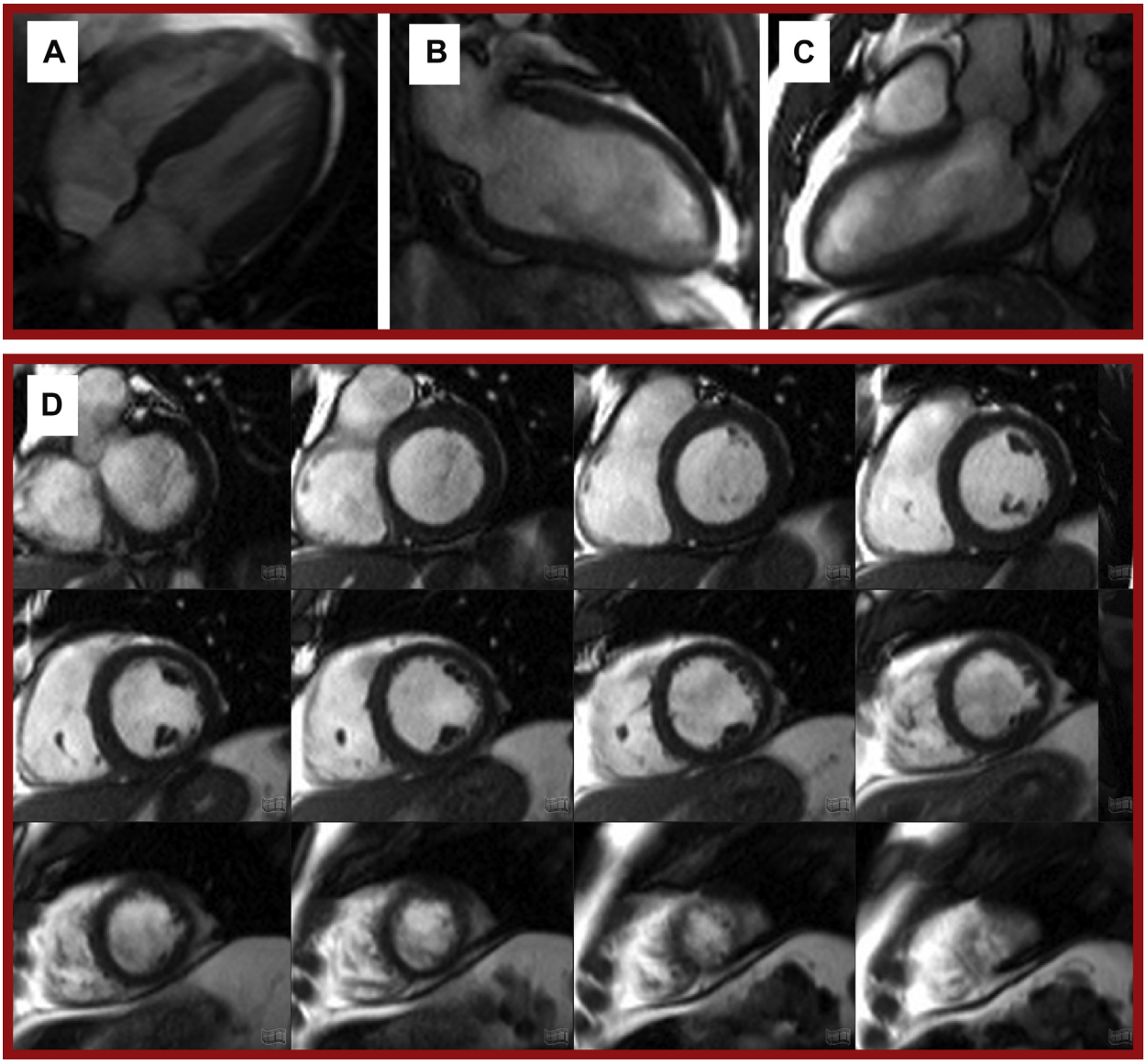

Example long-axis views: **(A)** 4-chamber, **(B)** 2-chamber, and **(C)** 3-chamber. **(D)** A stack of short axis "slices" from base to apex.

therefore appear markedly hypointense (dark) (**Figure 6**) on EGE sequences when surrounding structures appear hyperintense (bright).

The distribution of the contrast in the myocardium is also a function of the permeability of the tissue. In the setting of myocardial edema, there is enhanced vasodilatation and vascular permeability of inflamed tissue; EGE sequences have been used as a marker of myocardial injury in patients with myocarditis (23) and form part of the Lake Louise diagnostic criteria (25). In a study of 22 patients using EGE sequences, an increase in myocardial signal intensity 3 days after the administration of anthracyclines predicted subsequent declines in LVEF at 28 days (29).

MYOCARDIAL SCARRING/FIBROSIS: LGE SEQUENCES. LGE is the cornerstone of CMR tissue characterization and its presence predicts adverse outcomes in a variety of cardiomyopathies, including coronary artery disease (30), nonischemic cardiomyopathy (31),

FIGURE 5 **Feature Tracking Strain Overlay on Steady-State Free Precession Images of the Left Ventricle**

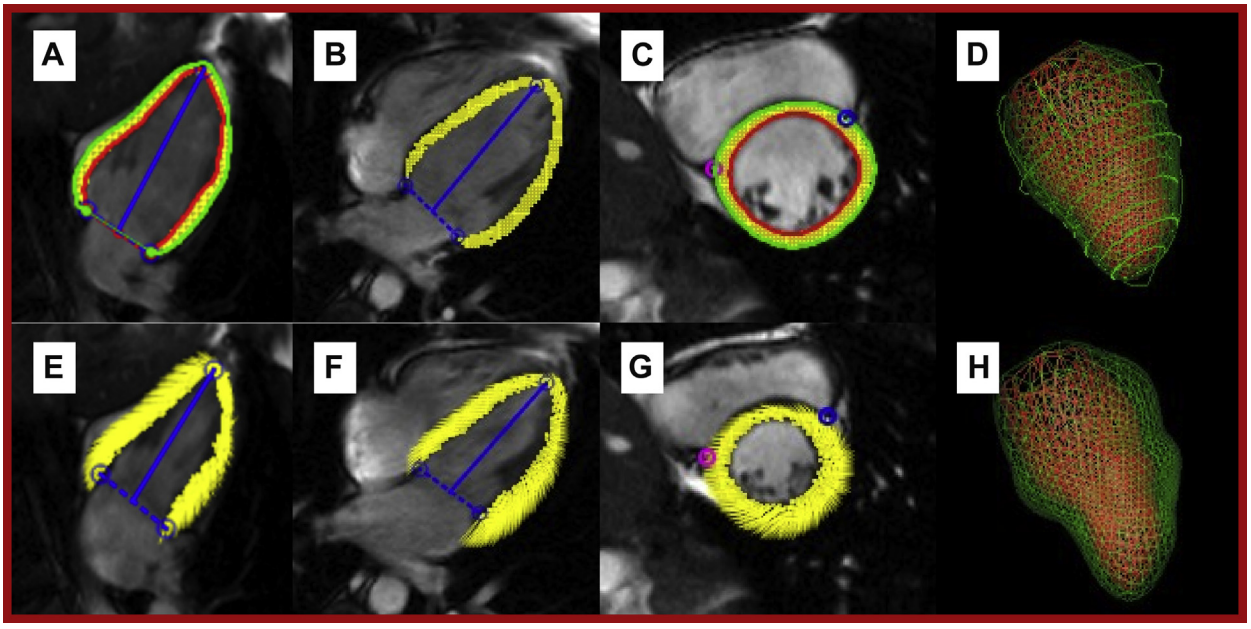

Diastole **(A to D)** and systole **(E to H).** A and E show a 2-chamber view. B and F show a 4-chamber view. C and G show a mid-ventricular short axis view. D and H show a composite 3-dimensional reconstruction. **Red line** represents endocardial border; **green** represents epicardial border; and **yellow** represents tracked myocardial features.

hypertrophic cardiomyopathy (32), cardiac sarcoidosis (33), myocarditis (34), and cardiac amyloidosis (35). Gadolinium preferentially accumulates in areas of interstitial expansion (typically scar and fibrosis) giving these areas a hyperintense (bright) appearance on T1-weighted sequences in comparison to surrounding healthy myocardium, which appears of lower signal intensity (darker) because of the comparative absence of contrast. The accumulation pattern of contrast in the myocardium mirrors the pathophysiology of the underlying disease, defining ischemic patterns (subendocardial or transmural, following the ischemic necrotic wave-front phenomenon) and nonischemic patterns (mid-wall, epicardial) (**Figure 7**). Data on the presence and distribution of LGE in human populations treated with anthracyclines are conflicting. Prospective CMR studies have generally reported the absence of new segments of LGE (18,36-38), whereas some studies report an incidence of between 23% (39) and 30% (40), with a mid-myocardial or subepicardial distribution described. Retrospective studies conducted over a longer period of follow-up in different populations have reported that LGE was an infrequent finding (41-43) that was associated with adverse left ventricular remodeling in 1 study (43). A histopathologic study of 10 explanted hearts with advanced anthracycline cardiomyopathy (1 mortality and 9 following cardiac transplant) reported interstitial fibrosis in all cases but with a spectrum of distributions: 6 with multifocal fibrosis, 3 with diffuse fibrosis, and 1 with focal fibrosis. A porcine model of anthracycline cardiotoxicity reported that LGE appeared relatively late and in a patchy distribution that became more apparent as time progressed (26).

INTRACELLULAR AND INTERSTITIAL MYOCARDIAL FIBROSIS AND EDEMA/INFLAMMATION: NATIVE T1 MAPPING AND EXTRACELLULAR VOLUME FRACTION SEQUENCES. Novel tissue characterization sequences such as native T1 mapping and extracellular volume (ECV) fraction estimation have shown promise to detect diffuse fibrosis and inflammation/edema by quantitatively assessing its presence and extent (**Figure 8**). When conducted in accordance with recognized guidelines (44), these techniques have shown excellent reproducibility and robust validation against biopsy-proven collagen volume fraction and extracellular space reported in explanted hearts (45)

FIGURE 6 Examples of Intracardiac Thrombus on CMR

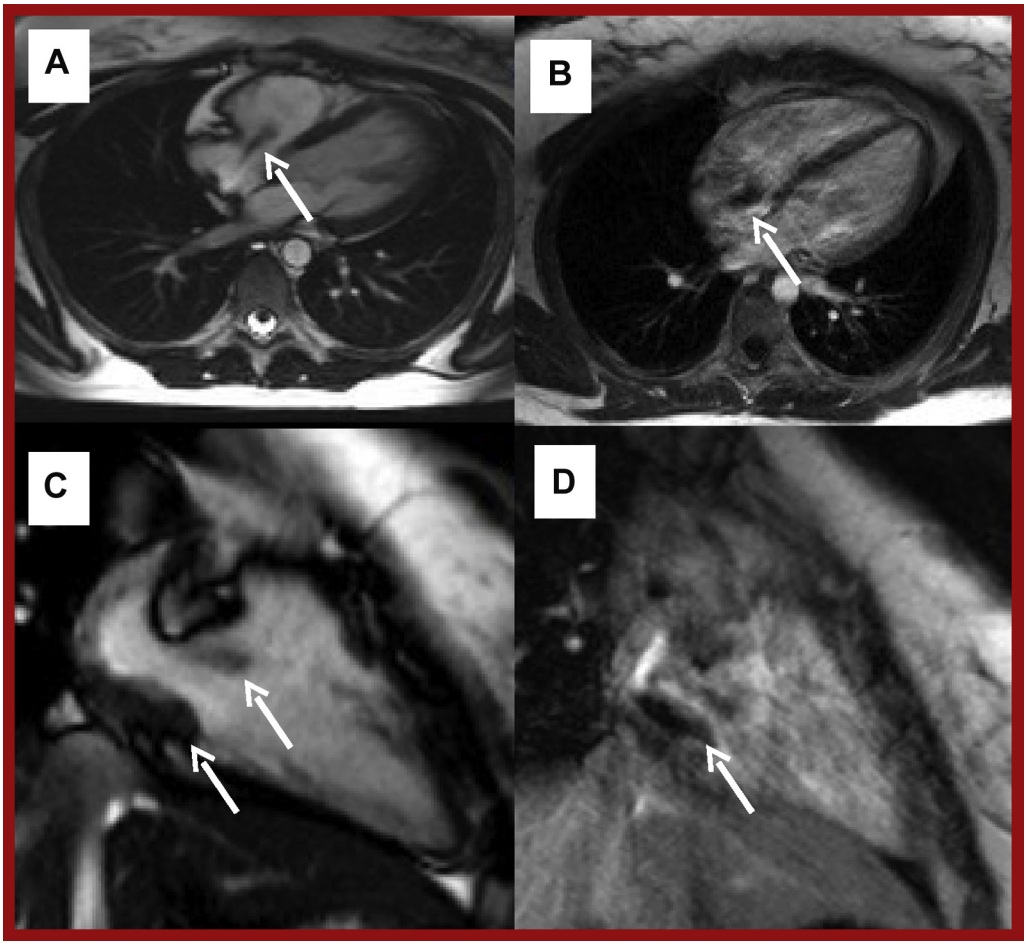

(A) Axial SSFP showing PICC-associated thrombus prolapsing through the tricuspid valve **(arrow). (B)** T1-weighted EGE image showing marked hypointensity of the same thrombus **(arrow). (C)** RV 2-chamber cine showing 2 separate thrombi **(arrows)** in the same patient. **(D)** T1-weighted RV 2-chamber EGE image of the same patient, with thrombus indicated by an **arrow.** EGE = early gadolinium enhancement; PICC = peripherally inserted central catheter; SSFP = steady-state free precession; other abbreviations as in Figure 1.

and biopsied patients with dilated cardiomyopathy (46). Using this technique, an increased ECV, used as a surrogate marker of myocardial fibrosis, was reported in a cohort of patients receiving anthracyclines, as compared to age- and sex-matched controls (47); this has also been shown to occur independently of underlying cancer or cardiovascular comorbidities 3 years after anthracycline treatment (48). However, a precise role for these sequences in the setting of cancer therapy is yet to be established, and the temporal variability of ECV and T1 mapping in healthy controls was comparable to that seen in patients receiving cancer therapy, which poses a challenge to routine clinical application (49).

BLOOD FLOW, VELOCITY, AND VOLUME: PHASE-CONTRAST SEQUENCES. Phase contrast or velocity-encoded sequences enable CMR to accurately assess and characterize blood flow, which is particularly relevant in valvular and congenital heart disease. Whereas echocardiography is the first-line imaging modality, CMR can provide complementary information where initial results are discrepant, of limited quality or not obtainable, or when an alternate imaging plane or additional information (e.g., myocardial viability) is required (50). In addition, vessel "stiffness" and distensibility can be assessed by phase-contrast imaging of the aorta. Aortic pulse wave velocity increases significantly in after

FIGURE 7 Patterns of Myocardial Scarring in Post-Contrast Images (Late Myocardial Enhancement)

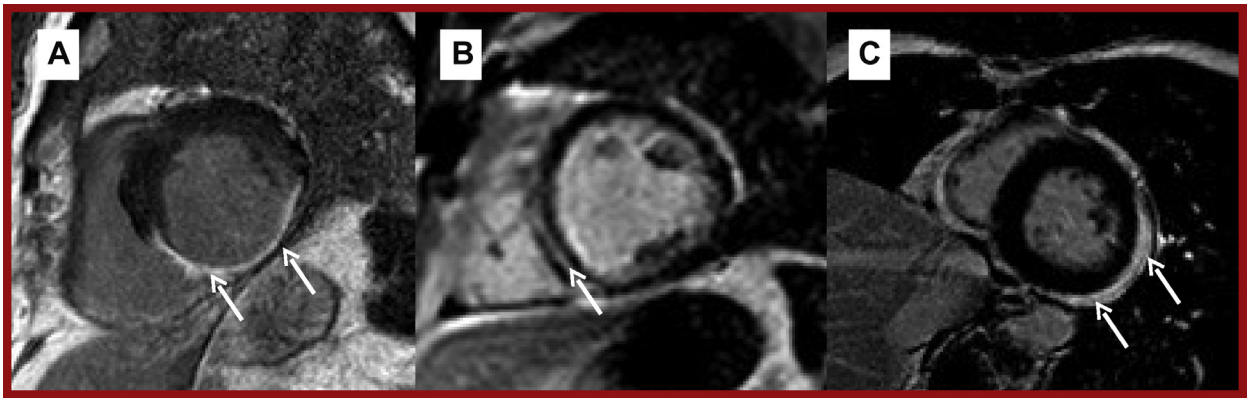

T1-weighted post-contrast short-axis mid ventricular images. **(A)** Ischemic LGE **(arrows)** due to transmural infarction in the right coronary artery territory. **(B)** Mid-myocardial LGE in dilated cardiomyopathy **(arrow)**. **(C)** Subepicardial LGE **(arrows).** LGE = late gadolinium enhancement.

anthracycline (18,51), although the impact on clinical outcomes in cardio-oncology populations is not known.

CLINICAL INDICATIONS FOR CMR

Diagnosis of cardiovascular disease during and after cancer therapy through symptoms alone can pose a diagnostic challenge to cardio-oncologists. This is because cardiovascular effects can manifest through a variety of overlapping symptoms (**Figure 9**) and are interpreted in the context of an underlying cancer diagnosis, which may itself express a significant symptom burden. In this regard, CMR can be a useful diagnostic tool. Furthermore, knowledge of cardiovascular effects according to therapeutic class, incidence, and time of onset can be invaluable. In the following paragraphs, we describe the relevant clinical indications for CMR in cardio-oncology patients. **Table 2** also summarizes these indications and

FIGURE 8 Native Short-Axis Mid-Ventricular T1 Map

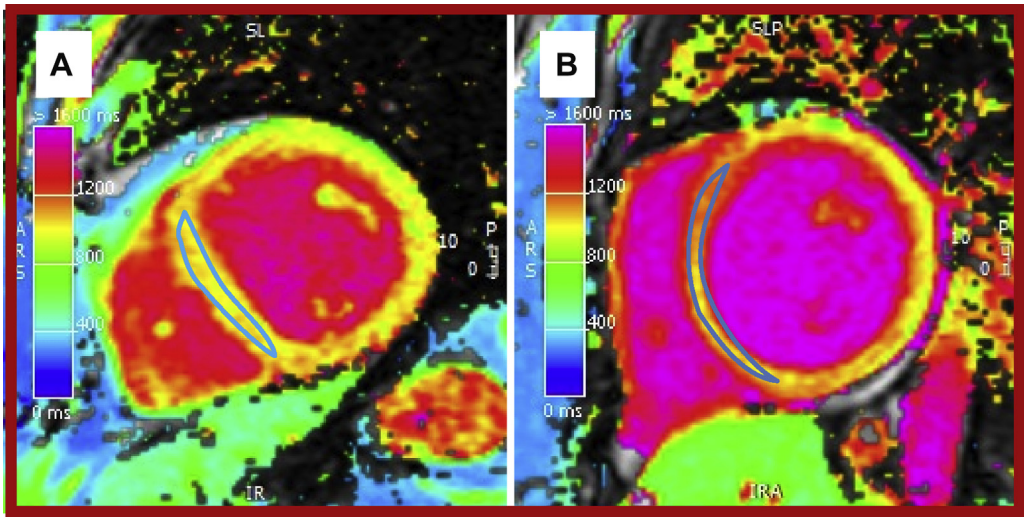

(A) Normal native myocardial measurements (1,010 ms) and **(B)** abnormal measurements (1,136 ms) in the mid-ventricular septum.

FIGURE 9 Overlapping Symptomatology of Cardiovascular Effects of Cancer Therapy

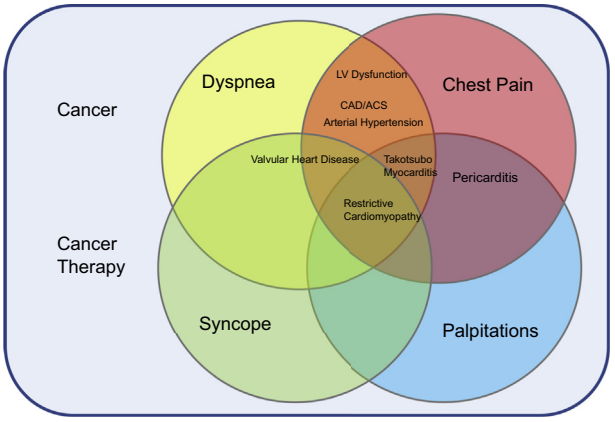

Cardiovascular effects of cancer therapy can manifest with a variety of cardiovascular symptoms and occur in the context of cancer and cancer therapy, which can themselves cause similar symptoms, independent of cardiovascular disease, highlighting the diagnostic challenges faced by cardio-oncologists. ACS = acute coronary syndrome; CAD = coronary artery disease.

includes the suggested protocol and data provided by each sequence.

MYOCARDIAL DYSFUNCTION AND HEART FAILURE. Left ventricular dysfunction that manifests clinically as heart failure is 1 of the most concerning complications of cancer therapy, not only because it may lead to cancer treatment interruption, but also because it carries an adverse prognosis, particularly when detected late (52).

In a porcine model of anthracycline toxicity, Galan-Arriola (26) has shown that T2 relaxation-time prolongation (a marker of edema) was the earliest CMR parameter to change. This occurred at week 6 (2 weeks after the third dose of intracoronary doxorubicin), corresponded with intracardiomyocyte edema at the tissue level, and importantly, identified toxicity at a reversible stage. Other parameters such as T1 mapping, ECV (markers of fibrosis), and left ventricular wall motion only occurred at a later stage, when fibrotic histologic changes became irreversible. These data are yet to be replicated in a human population but highlight the potential utility of T2 mapping to inform treatment and monitoring strategies.

Although the noninvasive evaluation of LVEF has several limitations, it is the most widely accepted strategy for monitoring cardiac function in cardio-oncology. With this in mind, it is important to understand that different mechanisms can drive changes in LVEF, which is a product of end-diastolic and end-systolic left ventricular volumes. One study of 120 adults reported that among patients with declines in LVEF meeting criteria for cardiotoxicity, 19% were due to an isolated decrease in end-diastolic volume, thought principally to represent volume depletion (53). Furthermore, declines in LVEF driven by an increase in end-systolic volume can be caused both by extrinsic factors such as increased afterload, as well as intrinsic myocardial dysfunction (54). These factors should be considered when interpreting CMR imaging results in patients receiving cancer therapy.

The precision of CMR in measuring dynamic changes in ventricular volumes and ventricular mass make it an important tool to monitor and identify early subtle cardiac changes associated with cancer therapy used by a number of prospective studies (**Table 3**) (55). From a clinical standpoint, it is particularly helpful in determining biventricular function in challenging cases (e.g., patients who have undergone left sided breast surgery or with LVEF results that are borderline or conflicting) or in determining the etiology of the cardiomyopathy (1,56).

Chimeric antigen receptor (CAR) T cell therapy is revolutionizing the treatment of relapsed or refractory hematologic malignancy and is likely to acquire other indications in time. Despite these advances, a significant complication is cytokine release syndrome, and the limited data describing cardiovascular involvement are of particular relevance. Cardiovascular manifestations include tachycardia, hypotension, troponin elevation, left ventricular dysfunction, pulmonary edema, and, in severe cases, cardiogenic shock; although for most patients with adequate physiologic reserve, the myocardial insult appears to be reversible (57). Data are currently limited to case reports and early clinical trials (58) but it is hoped that a prospective observational study addressing the cardiovascular effects of CAR T cell therapy will be instructive (NCT04026737). One pediatric study reported that impaired systolic and diastolic function before CAR-T were associated with subsequent hypotension requiring inotropic support (59). Although the use of CMR in the setting of CAR T cell therapy is, to the best of our knowledge, yet to be fully described, its unique ability to noninvasively assess acute cardiomyopathic processes mean that CMR is well placed to provide important insights, and led to its inclusion in a recently proposed screening and monitoring algorithm (60).

CMR is also a valuable tool to evaluate cardiomyopathy late after chemotherapy, which is particularly relevant when managing the increasing population of

TABLE 2 Protocols for Assessment of Specific Clinical Cardiotoxicity Indications

		Recommended Protocol and Parameters Reported								
		Anatomy	Cine	Edema	Native T1/T2	Perfusion* (± Stress)	EGE*	LGE*	PC T1*	Phase Contrast
Indication	Guideline Support	Descriptive	LVEDV (ml), LVESV (ml), LVEF (%), LVM (g), (FT-Strain [%])	Presence and Extent	Global/ Regional Values (ms)	Vascularity Presence of Hypoperfusion	Presence of Edema Presence of Thrombus	Presence and Extent of Scarring/ Fibrosis	ECV (%)	Flow (ml), Velocity (m/s), RF (%)
LV dysfunction										
Baseline evaluation	Yes (second-line)	✓	✓	✓	(✓)	± Stress	✓	✓	(✓)	
Serial evaluation	Yes (second-line)	✓	✓	±	(✓)					
Etiological evaluation	Yes (second-line)	✓	✓	✓	(✓)	± Stress	✓	✓	(✓)	
Myocarditis/TCM	Yes	✓	✓	✓	(✓)		✓	✓	(✓)	
restrictive	Yes	✓	✓	±	(✓)		✓	✓	(✓)	
CAD	Yes	✓	✓		(✓)	✓	✓	✓	(✓)	
VHD	Yes (second-line)	✓	✓		(✓)		±	±	(✓)	✓
Arterial hypertension	No	✓	✓		(✓)		✓	✓	(✓)	✓
Pericardium	Yes	✓	✓	±	(±)	±	✓	✓	(±)	✓

*Requires gadolinium contrast administration. ✓ = recommended, (✓) = aspirational, ± = can be included in appropriate clinical context; (±) = aspirational.

CAD = coronary artery disease; FT = feature tracking; LV = left ventricular; LVEDV = left ventricular end-diastolic volume; LVEF = left ventricular ejection fraction; LVESV = left ventricular end systolic volume; LVM = left ventricular mass; PC = postcontrast; RF = regurgitant fraction; TCM = Takotsubo cardiomyopathy; VHD = valvular heart disease; other abbreviations as in Table 1.

pediatric and adult cancer survivors. CMR identified a higher prevalence (14%) of cardiomyopathy (LVEF <50%) in 114 asymptomatic childhood cancer survivors assessed 27.8 years after anthracycline chemotherapy compared to 2D or 3D echocardiography (55). In fact, 11% of the study population was misclassified as having a normal LVEF by 2D echocardiography in comparison to CMR with the higher cutoffof 60% improving the detection of cardiomyopathy. In another study, 62 asymptomatic childhood cancer survivors were assessed a median of 7.8 years after anthracycline treatment; the prevalence of cardiomyopathy (ejection fraction <55%) in the right and left ventricles was 81% and 79%, respectively (61). A subsequent study by the same group using 2D and 3D echocardiography and CMR reported the prevalence of cardiomyopathy (LVEF <55%) as 78% in 71 survivors of childhood cancer (62).

In addition to the assessment of heart failure with reduced ejection fraction, accumulating evidence identifies a role for CMR in the challenging and heterogeneous cohort of patients with heart failure with preserved ejection fraction (63). A study of contemporary radiotherapy for breast cancer reported that the risk of heart failure with preserved ejection fraction increased with increasing cardiac radiation dose; the odds ratio per log mean cardiac radiation dose was 16.9 (95% confidence interval: 3.9 to 73.7) compared to controls (64). While echocardiography remains the cornerstone of assessing diastolic function, the ability of CMR to: 1) determine left atrial and left ventricular volumes; 2) derive dynamic time-volume filling curves; 3) assess flow in any plane (e.g., pulmonary vein and transmitral); 4) yield myocardial strain data; and 5) characterize the myocardium means that CMR can potentially add value to the diagnostic work-up and may also identify alternative pathologies (63).

Left ventricular mass is another CMR-derived marker of interest for quantifying cardiotoxicity. An inverse association between anthracycline dose and left ventricular mass was reported in a study of 91 patients with cardiomyopathy a median of 88 months after chemotherapy (41), which is in keeping with the report of Armstrong et al. (55) which found that 48% of patients had a left ventricular mass that was 2 standard deviations below normal. Furthermore, in the former study, left ventricular mass showed a strong inverse association with major adverse cardiovascular events (MACE). A recent report (65) provided additional pathophysiologic insight by suggesting that this decrease may be due to cardiomyocyte apoptosis.

MYOCARDITIS. CMR is a key noninvasive test for the diagnosis of myocarditis, with an approach that combines imaging sequences (e.g., T1 mapping and LGE) reported to improve sensitivity and specificity

TABLE 3 Selected Prospective Adult Human Studies of Cardiotoxicity Using CMR

First Author, Year (Ref. #)	N	Mean Age (yrs); % Female	Treatment	Follow-Up Imaging	Definition and Incidence of Cardiotoxicity	Findings
Wassmuth et al., 2001 (29)	22	43; 77%	First course: doxorubicin 67 mg/m^2 or epirubicin 76 mg/m^2	3 and 28 days after treatment initiation	LVEF <55% occurred in 27% (n = 6)	Significant decrease in LVEF 67.8 ± 1.4% to 58.9 ± 1.9%; LVEF decreased significantly at 28 days in patients with an increase in relative contrast enhancement of >5 on day 3
Chaosuwannakit et al., 2010 (51)	40	52; 70%	Doxorubicin 215 mg/m^2 or daunorubicin 265 mg/m^2 or trastuzumab 920 mg	4 months after treatment initiation	Not reported	Significant decrease in LVEF 58.6 ± 6.3% to 53.9 ± 6.4%; significant increase in aortic stiffness ($p < 0.0001$)
Fallah-Rad et al., 2011 (39)	42	47; 100%	Epirubicin or adriamycin, followed by trastuzumab	12 months after treatment initiation	LVEF decline of 10% to <55% occurred in 24% (n = 10); determined by echo	Significant decrease in LVEF 66 ± 5% to 47 ± 4% in 10 with cardiotoxicity, all of whom exhibited subepicardial LGE
Drafts et al., 2013 (18)	53	50; 58%	50-375 mg/m^2 doxorubicin equivalent	1, 3, and 6 months after treatment initiation	Of those with LVEF >50% at baseline (n = 47), 26% (n = 12) had LVEF <50% after 6 months	Significant decrease in LVEF 58 ± 1% to 53 ± 1%; significant decrease in mean mid wall circumferential strain (-17.7 ± 0.4% to -15.1 ± 0.4%; p = 0.0003) No new LGE
Jordan et al., 2014 (37)	65	51; 86%	55% (n = 36) received median 240 mg/m^2 doxorubicin equivalent, 38% (n = 25) received a monoclonal antibody	3 months after treatment initiation	Not reported	Significant decrease in LVEF 57 ± 6% to 54 ± 7%; significant increase in T1-weighted signal intensity 14.1 ± 5.1 to 15.9 ± 6.8 No LGE
Lunning et al., 2015 (40)	10	59; 40%	300 mg/m^2 doxorubicin	3 months after treatment completion	LVEF decrease by >10% occurred in 50%	Significant decrease in FT-GCS (p = 0.018); trend to FT-GLS decrease (p = 0.073) 30% exhibited 1 new or progressive segment of LGE
Nakano et al., 2016 (38)	9	62.3; 100%	67% had epirubicin; 100% had trastuzumab	3, 6, and 12 months after treatment initiation	No cardiotoxicity	Significant decrease in LVEF (68.4 ± 6.6% to 61.7 ± 8.7) at 6 and 12 months (62.9 ± 7.8%) but not at 3 months (65.4 ± 8.7%); significant decrease in SENC-GLS and SEND-GCS at 6 months but not at 3 or 12 months
Barthur et al., 2017 (114)	41	52; 100%	56% received anthracycline; 100% received 18 cycles of trastuzumab	6, 12, and 18 months	No cardiotoxicity	Significant decrease in LVEF at 6 (60.4 ± 4.2% to 58.3 ± 5.1%) and 12 (57.9 ± 4.8%) months but not at 18 months; significant decrease in RVEF at 6 (58.3% to 53.9%) and 12 (55%), which had recovered at 18 months (56.6%)
Muehlberg et al., 2018 (36)	23	59; 52%	360-40 mg/m^2 doxorubicin equivalent	48 h after treatment initiation and on treatment completion	LVEF decrease by >10% occurred in 39% (n = 9)	Significant decrease in subgroup with cardiotoxicity (63.5 ± 5.8% to 49.9 ± 5.0%) but not in those without cardiotoxicity (59.2 ± 10.3% to 58.3 ± 7.8%); at 48 h, the subgroup who developed cardiotoxicity had significantly lower native T1 times than those who did not
Ong et al., 2018 (20)	41	52; 100%	56% (n = 23) received anthracycline, 100% received trastuzumab	6, 12, and 18 months after treatment initiation	2.4% (n = 1) experienced cardiotoxicity	Significant decrease in LVEF at 6 months (60.4% to 58.4%) and 12 months (57.9%) but not at 18 months (60.2%); significant decrease in FT-GLS and FT-GCS at 6 and 12 months but not at 18 months

GCS = global circumferential strain; GLS = global longitudinal strain; RVEF = right ventricular ejection fraction; SENC = strain-encoded imaging; other abbreviations as in Tables 1 and 2.

(25). Immune checkpoint inhibitors (ICIs) have revolutionized cancer treatment, but their mechanism of action can lead to immune reactions against normal tissue, including the myocardium. ICI-associated myocarditis is a rare but serious side effect with an estimated incidence of 0.06% to 1.14%, and MACE rate of 46% in affected individuals (66) that occurs at a median of 34 days from treatment initiation (66).

In addition to being rare, ICI-associated myocarditis has a notoriously variable clinical presentation and until recently had no widely accepted definition. Furthermore, clinical practice guidelines on the

FIGURE 10 CMR and Angiographic Case Example of Ischemic Heart Disease

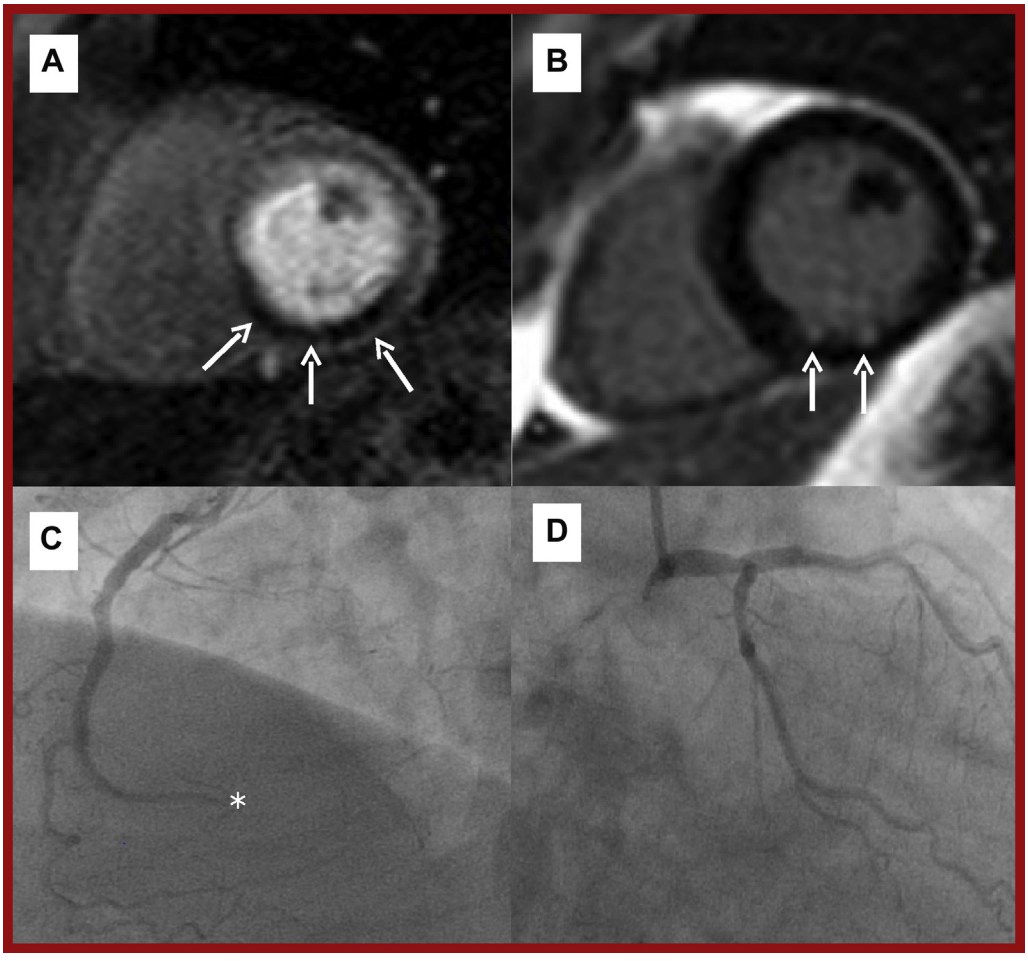

(A) T1-weighted mid-ventricular short-axis stress perfusion image showing an extensive inducible perfusion defect in the inferior and inferoseptal walls **(arrows). (B)** T1-weighted short-axis image showing minimal scar according to small volume of LGE **(arrows). (C)** Coronary angiography of the distally occluded (*) dominant right coronary artery. **(D)** Coronary angiography of the unobstructed left coronary artery. The left circumflex is recessive and the posterior descending and posterior left ventricular branches of the right coronary artery are missing. Abbreviations as in **Figures 1 and 7**.

management of ICI-associated myocarditis have not traditionally described a diagnostic role for CMR (67,68). However, more recently, Bonaca et al. (69) published a proposed definition of ICI-associated myocarditis describing CMR as the preferred imaging modality to establish the diagnosis. CMR findings of ICI-associated myocarditis have been described in 2 case series (66,70). In the first series of 35 cases, 27 (77%) patients exhibited LGE on CMR in a pattern typical of myocarditis (subepicardial [n = 6], mid-myocardial [n = 12], and diffuse [n = 9]), although the majority (51%) of these patients had a normal LVEF (66). In a large recent series of 103 patients with ICI-associated myocarditis evaluated with CMR, the mean LVEF was 50%, but the majority of patients (61%) had an LVEF >50% overall (70). LGE was present in 48% of the cohort overall; 55% in those with reduced LVEF; and 43% in those with preserved LVEF. The presence of LGE increased from 21.6% when CMR was performed within 4 days of admission to 72% when performed on day 4 or later. Fifty-one patients (40%) suffered from MACE over a follow-up of 5 months, although LGE was not predictive of MACE (70). Therefore, increasing awareness of this entity and recognition of the unique diagnostic capabilities of CMR may see its use in this setting

increase in the coming years. However, a normal CMR does not exclude ICI-associated myocarditis and critically ill patients may not be suitable for CMR scanning (71).

Takotsubo cardiomyopathy (TCM) is a clinical syndrome presenting with symptoms (chest pain) and objective evidence (electrocardiogram abnormalities, including ST-segment elevation, troponin rise, and segmental myocardial dysfunction) of a myocardial infarction (MI) but with unobstructed coronary arteries on angiography. It is characteristically precipitated by an emotional or physical stressor that leads to acute segmental dysfunction of the left ventricular apex, leading to "apical ballooning" morphology. Cancer therapies reported to trigger TCM include 5-flourouracil, capecitabine, rituximab, and ICIs, although a broad range of onset between 26 h and 3 months from treatment initiation has been reported (72). Patients with a history of malignancy may have a greater risk of developing Takotsubo (73), although the mechanisms underlying this are incompletely understood (54). In addition to the typical morphologic appearance of the left ventricle, TCM is readily identifiable on CMR by the presence of myocardial edema on T2-weighted imaging, elevated T2 mapping values, and the typical absence of fibrosis (LGE) (74).

CORONARY ARTERY DISEASE. CMR provides a comprehensive assessment of acute and chronic coronary artery disease presentations, which is recognized by international societal guidelines (75,76).

In the short term, cancer therapies such as fluoropyrimidines and platinum compounds can cause myocardial ischemia and infarction (1,56). CMR can readily detect MI and its complications (left ventricular thrombus, pseudoaneurysm, and microvascular obstruction) (77) and can be particularly helpful to assess patients with MI and nonobstructed coronary arteries (who often present a clinical dilemma).

In stable coronary artery disease, CMR can detect myocardial ischemia (**Figure 10**) and allows differentiation of viable from nonviable myocardium to inform coronary revascularization strategies when there is myocardial dysfunction (76). In a multicenter study of 918 patients with stable angina and risk factors for coronary artery disease, stress perfusion CMR was associated with a lower incidence of revascularization than invasive fractional flow reserve assessment (35.7% vs. 45.0%; $p = 0.005$, respectively) and was noninferior with respect to MACE at 1 year (3.6% vs. 3.7%, 95% CI: -2.7% to 2.4%) (78). It can also be used to risk-stratify asymptomatic patients with poor functional capacity and at least 2 clinical risk factors (ischemic heart disease, cerebrovascular disease, heart failure, diabetes mellitus requiring insulin, or renal dysfunction) before cancer surgery (79). Radiation-related coronary heart disease may not manifest for 15 to 20 years after treatment, and younger patients may be more susceptible (80). Furthermore, the risk of a major coronary events increases linearly with the mean cardiac radiotherapy dose (7.4% per Gray), starting 5 years after exposure (81). A higher prevalence of stress test abnormalities has been reported among women irradiated for left-sided breast cancer compared to right-sided breast cancer (82), and in a study of 31 patients assessed 24 years after treatment for Hodgkin's disease, 68% exhibited a perfusion defect (83). Stem cell transplantation is associated with accelerated cardiovascular disease in later life, with a 22% incidence of cerebrovascular disease, coronary artery disease, and/or peripheral arterial disease at 25 years in a single-center study of 265 long-term survivors (84).

VALVULAR HEART DISEASE. Chemotherapeutic agents do not typically affect heart valves (1,56), although valvular heart disease is clearly encountered in patients with cancer. Thoracic radiation increases the risk of cardiovascular disease (85), with valvular heart disease reported to affect 6.2% of Hodgkin lymphoma patients 22 years after treatment and an observed-to-expected ratio for valve surgery of 8.3 in 1 study (86). In a separate CMR study of 31 patients assessed 24 years after radiotherapy (mean dose, 40 Gray), the prevalence of hemodynamically significant valvular dysfunction was 42% (83). However, these risks are somewhat mitigated by modern radiotherapy dosing and administration techniques (87).

In the assessment of valvular heart disease, echocardiography is typically the first-line imaging investigation, but CMR can provide complementary information and is particularly useful when echocardiographic findings are inconclusive, discrepant, or not available (1,50). Using a combination of sequences, detailed anatomical and functional information about valve morphology (e.g., cuspidity and leaflet thickness) and the presence, location, and severity of valvular heart disease can be assessed either by estimating valve area and transvalvular gradient, or regurgitant volume and regurgitant fraction for stenotic and regurgitant lesions, respectively (85). Phase-contrast assessment of aortic stenosis has shown good agreement with both Doppler measurements (88) and invasive hemodynamic data (89). In addition to quantifying the severity of valve disease, CMR provides a precise estimation of its hemodynamic

consequences and relationship with the structure and function of the heart and great vessels. Stroke volume data from cine imaging can also be used to estimate regurgitant fraction and shunt volumes (50).

ARTERIAL HYPERTENSION. Hypertension is a highly prevalent, modifiable cardiovascular risk factor whose presence in combination with other comorbidities was identified as an important independent prognostic factor of survival in a study of 19,268 cancer patients (90). Certain cancer therapies, such as vascular endothelial growth factor inhibitors and tyrosine kinase inhibitors, increase the risk of incident hypertension and destabilization of previously controlled hypertension (1,56). In a meta-analysis of sorafenib, the overall incidence of hypertension was 23.4%, with 5.7% experiencing high-grade hypertension (91).

CMR can play an important role in the assessment of the cardiovascular consequences (e.g., left ventricular hypertrophy and fibrosis) of hypertension (92) and also in the exclusion of underlying secondary causes (renal artery stenosis and adrenal masses), although dedicated sequences, such as magnetic resonance angiography in the case of renal artery stenosis, would be required because they are not part of a standard CMR protocol but rather part of general scanning.

PERIPHERAL VASCULAR DISEASE. Cancer therapies such as tyrosine kinase inhibitors have been associated with the occurrence of peripheral vascular disease and adverse vascular events. Although the reported incidence varies considerably, it may be particularly high with some of the second- and third-generation tyrosine kinase inhibitors, such as nilotinib and ponatinib (93). Radiation-induced vascular disease appears histopathologically similar to atherosclerotic vascular disease including lipid deposition, inflammation, and thrombosis (94).

Contrast-enhanced angiography is a widely used and effective technique to evaluate both the central and peripheral vasculature that permits the anatomical characterization of vascular lesions and assessment of hemodynamic influence by phase-contrast or velocity-encoded CMR (85). These sequences would require a specific request because they are not included in a typical CMR protocol.

PERICARDIAL DISEASE. CMR is 1 of the most versatile modalities to evaluate pericardial disease, which in the field of cardio-oncology principally relates to pericardial thickening, pericardial inflammation and effusion, pericardial masses and in the late stages, pericardial constriction. Pericarditis has been reported to occur 2 to 145 months after radiotherapy with an absolute cumulative incidence of 2% to 5% (1,56) and occasionally follows an immediate and severe course, including large effusions and tamponade. Pericarditis is also a recognized side effect of chemotherapeutic agents such as doxorubicin, cytarabine, bleomycin, and cyclophosphamide (95) and may or may not be accompanied by myocarditis and pericardial effusion. Furthermore, cardiac graft-versus-host disease following allogenic stem cell transplantation may lead to pericardial effusions, tamponade, and constriction, with significant pericardial effusions identified in 4.4% of 205 patients at a median of 30 days in 1 study (96).

By combining anatomical information, tissue characterization, and detailed functional assessment, a comprehensive assessment of the pericardium and its hemodynamic consequences on ventricular filling is provided by CMR (97). This can be particularly helpful when results from echocardiography are inconclusive (95). Abnormal pericardial thickening (>3 mm) can accurately be defined by CMR and the signal intensity and late enhancement characteristics, with or without fat saturation, provides additional diagnostic information, for example, in distinguishing pericardial inflammation from pericardial fat (98). The presence, extent, and hemodynamic influence of accompanying pericardial effusion is readily detected by CMR with effusions as small as 30 ml reported to be detectible (97), although echocardiography is the first-line imaging modality to detect pericardial effusions. Pericardial calcification is best detected by computerized tomography, although its presence can also be suggested by very low signal intensity on CMR.

In the evaluation of pericardial constriction, CMR is reported to be 88% sensitive and 100% specific (99). A real-time short-axis mid-ventricular slice that typically spans 2 respiratory cycles is recommended with abnormal diastolic septal flattening during inspiration, giving a D-shaped appearance to the left ventricle, being indicative of constrictive physiology (98) (**Figure 11**).

RESTRICTIVE CARDIOMYOPATHY. Restrictive cardiomyopathy is a condition characterized by stiffness of the ventricular walls, which can be caused either by myocardial infiltration (e.g., amyloid), or in the case of radiation-induced cardiomyopathy, myocardial replacement fibrosis (100).

The inherent risks of invasive cardiac biopsy tend to preclude its routine clinical use in the assessment of restrictive cardiomyopathy, but with tissue characterization sequences (LGE, T1 mapping, and ECV),

FIGURE 11 CMR Case Example of Pericardial Constriction

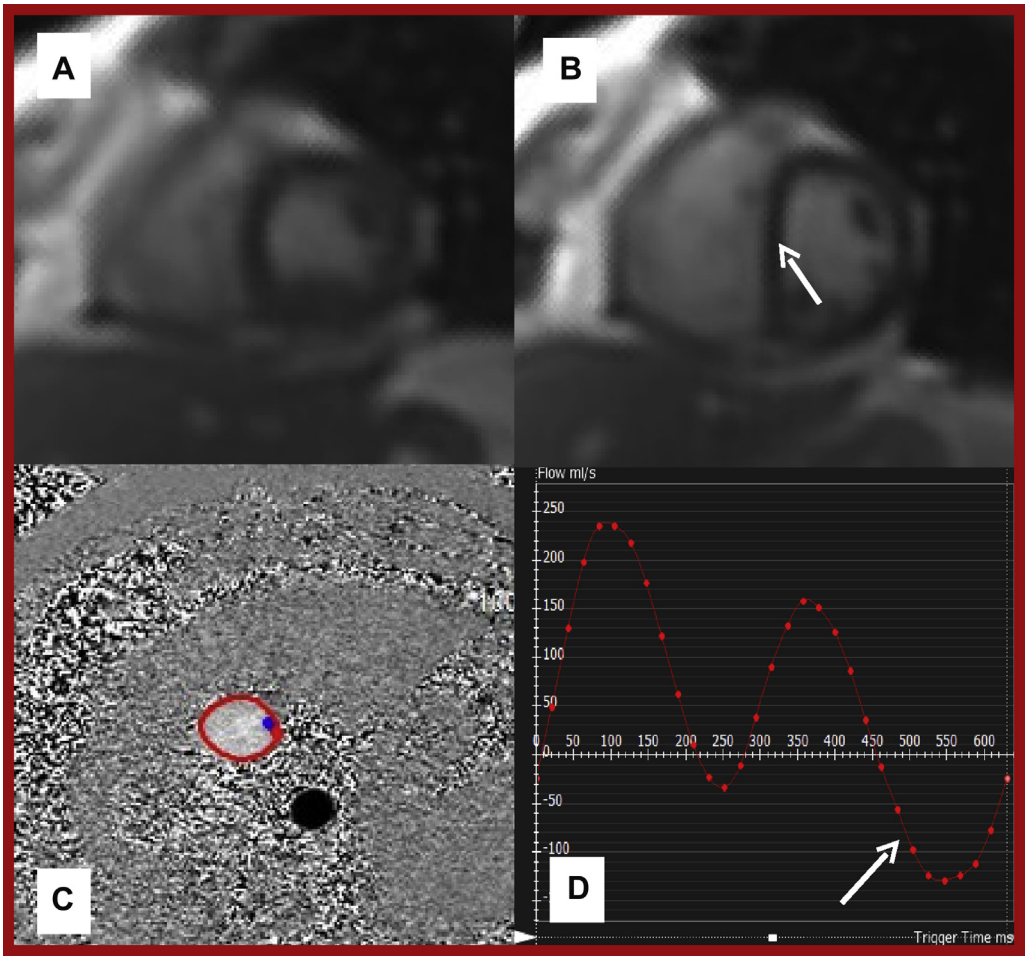

Real-time short-axis mid-ventricular SSFP cine imaging during deep breathing **(A)** during expiration, and **(B)** at onset of inspiration. Note the D-shaped LV due to septal flattening **(arrow). (C)** Axial phase-contrast imaging of the inferior vena cava, with a flow pattern **(D)** showing rapid and steep y descent with flow reversal in diastole **(arrow)** reminiscent of the jugular venous waveform encountered in pericardial constriction. Abbreviations as in **Figures 1 and 6**.

CMR can assess the myocardium noninvasively (101). Amyloid light chain amyloid, in particular, can result in cardiac involvement leading to a form of restrictive cardiomyopathy. Cardiac amyloid is readily detectible by CMR due to the interstitial deposition of amyloid proteins (elevated native T1 and elevated ECV are typical) (102,103). Patients with cardiac amyloidosis also have markedly abnormal gadolinium kinetics and a characteristic pattern of fibrosis (global subendocardial LGE) (104), which may permit the discrimination of amyloid from other wall-thickening disorders. In addition, difficulty in obtaining myocardial nulling (myocardium appears black), despite a T1 scout, may suggest underlying amyloid. However, although these techniques are sensitive, they are not specific to amyloidosis and do not obviate the need for a definitive histologic diagnosis (105).

CURRENT INTERNATIONAL GUIDELINE RECOMMENDATIONS ON THE ROLE OF CMR IN CARDIO-ONCOLOGY

CMR is becoming increasingly incorporated into societal cardio-oncology guidelines. The role identified for CMR in the most recent publications is described in detail below. In brief, CMR is particularly useful when LVEF is difficult to obtain by other means (106) (e.g., poor echocardiographic window due to left-sided breast surgery); when results obtained by other means are suboptimal, borderline, or conflicting

(95); and where discontinuation of chemotherapy is being contemplated (95). Furthermore, CMR is particularly useful in the assessment of pericardial disease (1,95), infiltrative diseases, and cardiac masses (1,95), as well as in determining the etiology of left ventricular dysfunction and presence of scarring or fibrosis (1).

EUROPEAN SOCIETY OF CARDIOLOGY POSITION PAPER ON CANCER TREATMENTS AND CARDIOVASCULAR TOXICITY. When considering strategies for screening and detecting cardiotoxicity, the choice of modality depends on local expertise and availability but the ESC describes several core principles, all of which are fulfilled by CMR (1):

- The same imaging modality and/or biomarker assay should be used for continued screening throughout the treatment pathway. Switching between modalities is strongly discouraged.
- Modalities and tests with the best reproducibility are preferred.
- Imaging modalities that provide additional relevant clinical information are preferred (e.g., right ventricular function, pulmonary pressures, valvular function, and pericardial evaluation).
- High-quality radiation-free imaging is preferred, if available.

In addition:

- CMR is useful to determine the cause of left ventricular dysfunction and to clarify left and right ventricular function in challenging cases (i.e., borderline or contradictory results from other imaging modalities).
- CMR also serves to evaluate the pericardium, especially in patients with chest irradiation.
- LGE may be useful to detect scarring or fibrosis, which may have prognostic implications in the context of impaired left ventricular function.

CMR is an excellent test for the comprehensive evaluation of cardiac masses and infiltrative conditions.

EXPERT CONSENSUS FOR MULTIMODALITY IMAGING EVALUATION OF ADULT PATIENTS DURING AND AFTER CANCER THERAPY: AMERICAN SOCIETY OF ECHOCARDIOGRAPHY AND THE EUROPEAN ASSOCIATION OF CARDIOVASCULAR IMAGING.

- CMR may be particularly useful in situations in which discontinuation of chemotherapy is being entertained and/or when there is concern regarding echocardiographic or equilibrium radionuclide angiographic calculation of LVEF (95).
- If the quality of the echocardiogram is suboptimal, CMR is recommended.
- CMR should be considered in evaluation of primary tumors of the heart with or without compromise of the pericardium or when the diagnosis of constrictive pericarditis remains uncertain after a careful echocardiographic evaluation.
- Standard precautions for CMR safety need to be followed, including consideration of electromagnetic interference. This may be particularly relevant in patients with breast cancer, who had tissue expanders placed for breast reconstruction may represent a hazard.

PREVENTION AND MONITORING OF CARDIAC DYSFUNCTION IN SURVIVORS OF ADULT CANCERS: AMERICAN SOCIETY OF CLINICAL ONCOLOGY CLINICAL PRACTICE GUIDELINE 2017. Imaging modalities such as CMR or multigated acquisition may be considered if an echocardiogram is not available or technically feasible (e.g., poor image quality as a result of body habitus, chronic lung conditions, or history of mediastinal surgery), with preference given to CMR (106).

CHALLENGES AND SAFETY IN CMR

CMR emerged as an important tool to evaluate the cardiovascular system nearly 2 decades ago, but significant barriers to its widespread use in routine clinical practice persist. CMR remains a comparatively time-consuming and complex investigation that is typically performed in academic centers. It requires a cooperative patient, ideally in sinus rhythm, who can hold his or her breath to provide high-quality images. However, the advent of novel technologies such as compressed sensing real-time cine CMR, self-gating, and artificial intelligence have the potential to simplify and reduce image acquisition time up to 20-fold without compromising image quality (107). The cost and general availability of MRI scanners is an additional problem that may partially be addressed by collaborative use of resources and establishment of referral pathways between smaller and larger institutions. Furthermore, most MRI scanners installed in the last 10 years have the capacity to undertake cardiac imaging. Data indicate that use of CMR has continued to increase in the United States during this period (108), with more than 600 centers submitting claims for CMR services according to 2018

TABLE 4 Safety Concerns in CMR and Possible Solutions

Category	Safety Concern	Possible Solution
MRI		
	Metallic foreign bodies (nonclinical)	Removal; Intra-orbital metallic foreign bodies are an absolute contraindication to MRI scanning.
	Metallic foreign bodies (clinical)	Patients with MRI-conditional devices that pose no hazard in specific conditions can safely undergo MRI scanning. Consult MRI safety of specific product or device (e.g. mrisafety.com). There is increasing evidence that the risks attached to previously MRI-unsafe clinical devices (e.g., legacy pacemakers, defibrillators, implantable loop recorders, and tissue expanders) can be mitigated and that patients can safely undergo MRI scanning (115,116). Consult MRI safety of specific product or device (e.g., mrisafety.com) and consult individuals/centers with expertise.
	Pregnancy	Often avoided during first trimester, although risk is not known. No known risk during second or third trimester.
Gadolinium contrast		
	Allergy	Gadolinium panel allergy testing.
	Anaphylaxis	Noncontrast study.
	Pregnancy	American College of Obstetricians and Gynecologists recommend that use should be limited to cases where diagnostic performance is significantly improved and is expected to improve fetal or maternal outcome.
	Breast feeding	American College of Obstetricians and Gynecologists recommend that breastfeeding should not be interrupted after gadolinium administration.
	Renal impairment	Weigh benefit and risk, minimize dose of a low-risk agent, avoid repeat dose for 7 days.
	Hemodialysis	Noncontrast study; dialyze within 24 h of administration if benefit believed to outweigh risk.

MRI = cardiac magnetic resonance; other abbreviation as in Table 1.

billing data furnished by the Centers for Medicare and Medicaid Services.

There is an increasing number of physicians (cardiologists and radiologists) who are training and certifying worldwide, and CMR expertise at both the clinician and technologist level is increasing. To increase availability of technology and expertise, the development of technologies that allow remote supervision (109) of CMR scanners may also have an important role to play in training staff in geographically remote locations. Shortened, simplified protocols (e.g., 15-min noncontrast cine study for ventricular dimensions and systolic function) coupled with increasing automation of acquisition, processing, and analysis, as well as the potential for remote collaboration, image analysis, and interpretation will also increase the accessibility of this important tool to clinicians working in a variety of health care settings.

Technical challenges in CMR can often be overcome. For example, CMR may be facilitated in claustrophobic patients with a prone position, use of an

TABLE 5 Relative Strengths and Limitations of Cardiovascular Imaging Modalities

	CMR	Echocardiography	Nuclear	CT
Advantages				
	Accuracy Reproducibility Tissue characterization Lack of radiation Morphological, functional and extra-cardiac information Multiplanar	Availability Safety Morphological and functional information Lack of radiation Low cost	Reproducibility Availability	Availability Scan time Spatial resolution Morphological and extra-cardiac information Low cost Multiplanar
Limitations				
	Availability Relative high cost Contrast reactions (rare) Renal impairment due to very rare risk (likely <0.07%) of nephrogenic systemic fibrosis with gadolinium (117)	Acoustic window Interobserver, intraobserver and interscan variability	Radiation exposure Limited morphological and functional information	Radiation exposure Limited functional information Contrast reactions Renal impairment due to risk of contrast-induced nephropathy

CT = computed tomography; other abbreviation as in Table 1.

eye mask, preprocedural sedative or general anesthetic (generally pediatric populations), or the accompaniment of a friend or relative or by using a large bore scanner. Difficulty breath-holding can be overcome by reducing the number of slices or phases and thus the time required for acquisition, by using a respiratory navigator, or by acquiring images during free breathing or inspiration, rather than held expiration. Traditionally, CMR exams have lasted approximately 60 min; however, the adoption of shortened protocols (3) can reduce this to 20 to 25 min without compromising image acquisition quality while maximizing patient comfort and efficiency. Image quality can be improved in patients with arrhythmia by using arrhythmia rejection and/or correction protocols, or by using prospective electrocardiogram gating or real-time acquisition. **Table 4** describes safety concerns and proposed solutions encountered in clinical CMR and **Table 5** describes relative strengths and limitations of each imaging modality.

CONCLUSIONS

Cardio-oncology is a diverse and rapidly evolving field. CMR provides comprehensive, accurate, and reproducible cardiovascular data that can be applied to a wide variety of clinical scenarios encountered by the cardio-oncologist. The use of CMR in this setting is supported by international societal guidance and an expanding evidence base. Barriers to the widespread use of CMR persist, although technological advances and stakeholder collaboration will improve access to and awareness of this increasingly indispensable investigation in modern medicine.

ADDRESS FOR CORRESPONDENCE: Dr. Chiara Bucciarelli-Ducci, Bristol Heart Institute, University Hospitals Bristol NHS Foundation Trust, Upper Maudlin Street, Bristol BS2 8HW, United Kingdom. E-mail: C.Bucciarelli-Ducci@bristol.ac.uk. Twitter: @chiarabd, @juancplana.

REFERENCES

1. Zamorano JL, Lancellotti P, Rodriguez Muñoz D, et al. 2016 ESC Position Paper on cancer treatments and cardiovascular toxicity developed under the auspices of the ESC Committee for Practice Guidelines: The Task Force for cancer treatments and cardiovascular toxicity of the European Society of Cardiology (ESC). Eur Heart J 2016;37:2768–801.

2. Doherty JU, Kort S, Mehran R, et al. ACC/AATS/AHA/ASE/ASNC/HRS/SCAI/SCCT/SCMR/STS 2019 appropriate use criteria for multimodality imaging in the assessment of cardiac structure and function in nonvalvular heart disease: a report of the American College of Cardiology Appropriate Use Criteria Task Force, American Association for Thoracic Surgery, American Heart Association, American Society of Echocardiography, American Society of Nuclear Cardiology, Heart Rhythm Society, Society for Cardiovascular Angiography and Interventions, Society of Cardiovascular Computed Tomography, Society for Cardiovascular Magnetic Resonance, and the Society of Thoracic Surgeons. J Am Coll Cardiol 2019;73:488–516.

3. Kramer CM, Barkhausen J, Bucciarelli-Ducci C, Flamm SD, Kim RJ, Nagel E. Standardized cardiovascular cardiac magnetic resonance (CMR) protocols: 2020 update. J Cardiovasc Magn Reson 2020;22:17.

4. Schulz-Menger J, Bluemke DA, Bremerich J, et al. Standardized image interpretation and post-processing in cardiovascular magnetic resonance — 2020 update: Society for Cardiovascular Magnetic Resonance (SCMR): Board of Trustees Task Force on Standardized Post-Processing. J Cardiovasc Magn Reson 2020;22:19.

5. Hundley WG, Bluemke D, Bogaert JG, et al. Society for Cardiovascular Magnetic Resonance guidelines for reporting cardiovascular magnetic resonance examinations. J Cardiovasc Magn Reson 2009;11:5.

6. Dunet V, Schwitter J, Meuli R, Beigelman-Aubry C. Incidental extracardiac findings on cardiac MR: systematic review and meta-analysis. J Magn Reson Imaging 2016;43:929–39.

7. Grothues F, Smith GC, Moon JC, et al. Comparison of interstudy reproducibility of cardiovascular magnetic resonance with two-dimensional echocardiography in normal subjects and in patients with heart failure or left ventricular hypertrophy. Am J Cardiol 2002;90:29–34.

8. Bellenger NG, Burgess MI, Ray SG, et al. Comparison of left ventricular ejection fraction and volumes in heart failure by echocardiography, radionuclide ventriculography and cardiovascular magnetic resonance; are they interchangeable? Eur Heart J 2000;21:1387–96.

9. Mooij CF, de Wit CJ, Graham DA, Powell AJ, Geva T. Reproducibility of MRI measurements of right ventricular size and function in patients with normal and dilated ventricles. J Magn Reson Imaging 2008;28:67–73.

10. Clarke CJ, Gurka MJ, Norton PT, Kramer CM, Hoyer AW. Assessment of the accuracy and reproducibility of RV volume measurements by CMR in congenital heart disease. J Am Coll Cardiol Img 2012;5:28–37.

11. Schulz-Menger J, Bluemke DA, Bremerich J, et al. Standardized image interpretation and post processing in cardiovascular magnetic resonance: Society for Cardiovascular Magnetic Resonance (SCMR) board of trustees task force on standardized post processing. J Cardiovasc Magn Reson 2013;15:35.

12. Cerqueira MD, Weissman NJ, Dilsizian V, et al. Standardized myocardial segmentation and nomenclature for tomographic imaging of the heart. A statement for health care professionals from the Cardiac Imaging Committee of the Council on Clinical Cardiology of the American Heart Association. Circulation 2002;105:539–42.

13. Gulati G, Heck SL, Ree AH, et al. Prevention of cardiac dysfunction during adjuvant breast cancer therapy (PRADA): a 2 × 2 factorial, randomized, placebo-controlled, double-blind clinical trial of candesartan and metoprolol. Eur Heart J 2016;37:1671–80.

14. Pituskin E, Mackey JR, Koshman S, et al. Multidisciplinary Approach to Novel Therapies in Cardio-Oncology Research (MANTICORE 101-Breast): a randomized trial for the prevention of trastuzumab-associated cardiotoxicity. J Clin Oncol 2017;35:870–7.

15. Romano S, Judd RM, Kim RJ, et al. Association of feature-tracking cardiac magnetic resonance left ventricular global longitudinal strain with all-cause mortality in patients with reduced left ventricular ejection fraction. Circulation 2017;135:2313–5.

16. Thavendiranathan P, Poulin F, Lim KD, Plana JC, Woo A, Marwick TH. Use of myocardial strain imaging by echocardiography for the early detection of cardiotoxicity in patients during and after cancer chemotherapy: a systematic review. J Am Coll Cardiol 2014;63:2751–68.

17. Negishi T, Thavendiranathan P, Negishi K, Marwick TH. Rationale and Design of the Strain Surveillance of Chemotherapy for Improving Cardiovascular Outcomes: the SUCCOUR trial. J Am Coll Cardiol Img 2018;1:1098–105.

18. Drafts BC, Twomley KM, D'Agostino R, et al. Low to moderate dose anthracycline-based

chemotherapy is associated with early noninvasive imaging evidence of subclinical cardiovascular disease. J Am Coll Cardiol Img 2013;6:877–85.

19. Jolly MP, Jordan JH, Meléndez GC, McNeal GR, D'Agostino RB, Hundley WG. Automated assessments of circumferential strain from cine CMR correlate with LVEF declines in cancer patients early after receipt of cardio-toxic chemotherapy. J Cardiovasc Magn Reson 2017;19:59.

20. Ong G, Brezden-Masley C, Dhir V, et al. Myocardial strain imaging by cardiac magnetic resonance for detection of subclinical myocardial dysfunction in breast cancer patients receiving trastuzumab and chemotherapy. Int J Cardiol 2018;261:228–33.

21. Erley J, Genovese D, Tapaskar N, et al. Echocardiography and cardiovascular magnetic resonance based evaluation of myocardial strain and relationship with late gadolinium enhancement. J Cardiovasc Magn Reson 2019;2:46.

22. Ugander M, Bagi PS, Oki AJ, et al. Myocardial edema as detected by pre-contrast T1 and T2 CMR delineates area at risk associated with acute myocardial infarction. J Am Coll Cardiol Img 2012;5:596–603.

23. Friedrich MG, Sechtem U, Schulz-Menger J, et al. Cardiovascular magnetic resonance in myocarditis: A JACC White Paper. J Am Coll Cardiol 2009;53:1475–87.

24. McAlindon E, Pufulete M, Lawton C, Angelini GD, Bucciarelli-Ducci C. Quantification of infarct size and myocardium at risk: evaluation of different techniques and its implications. Eur Heart J Cardiovasc Imaging 2015;16:738–46.

25. Ferreira VM, Schulz-Menger J, Holmvang G, et al. Cardiovascular magnetic resonance in nonischemic myocardial inflammation: expert recommendations. J Am Coll Cardiol 2018;72:3158–76.

26. Galán-Arriola C, Lobo M, Vílchez-Tschischke JP, et al. Serial cardiac magnetic resonance to identify early stages of anthracycline-induced cardiotoxicity. J Am Coll Cardiol 2019;73:779–91.

27. Haslbauer JD, Lindner S, Valbuena-Lopez S, et al. CMR imaging biosignature of cardiac involvement due to cancer-related treatment by T1 and T2 mapping. Int J Cardiol 2019;275:179–86.

28. Motwani M, Kidambi A, Herzog BA, Uddin A, Greenwood JP, Plein S. MR imaging of cardiac tumors and masses: a review of methods and clinical applications. Radiology 2013;268:26–43.

29. Wassmuth R, Lentzsch S, Erdbruegger U, et al. Subclinical cardiotoxic effects of anthracyclines as assessed by cardiac magnetic resonance-a pilot study. Am Heart J 2001;141:1007–13.

30. Kwong RY, Chan AK, Brown KA, et al. Impact of unrecognized myocardial scar detected by cardiac magnetic resonance on event-free survival in patients presenting with signs or symptoms of coronary artery disease. Circulation 2006;113:2733–43.

31. Wu KC, Weiss RG, Thiemann DR, et al. Late gadolinium enhancement by cardiovascular magnetic resonance heralds an adverse prognosis in nonischemic cardiomyopathy. J Am Coll Cardiol 2008;51:2414–21.

32. O'Hanlon R, Grasso A, Roughton M, et al. Prognostic significance of myocardial fibrosis in hypertrophic cardiomyopathy. J Am Coll Cardiol 2010;56:867–74.

33. Hulten E, Agarwal V, Cahill M, et al. Presence of late gadolinium enhancement by cardiac magnetic resonance among patients with suspected cardiac sarcoidosis is associated with adverse cardiovascular prognosis: a systematic review and meta-analysis. Circ Cardiovasc Imaging 2016;9:e005001.

34. Gräni C, Eichhorn C, Bière L, et al. Prognostic value of cardiac magnetic resonance tissue characterization in risk stratifying patients with suspected myocarditis. J Am Coll Cardiol 2017;70:1964–76.

35. Fontana M, Pica S, Reant P, et al. Prognostic value of late gadolinium enhancement cardiovascular magnetic resonance in cardiac amyloidosis. Circulation 2015;132:1570–9.

36. Muehlberg F, Funk S, Zange L, et al. Native myocardial T1 time can predict development of subsequent anthracycline-induced cardiomyopathy. ESC Heart Fail 2018;5:620–9.

37. Jordan JH, D'Agostino RB, Hamilton CA, et al. Longitudinal assessment of concurrent changes in left ventricular ejection fraction and left ventricular myocardial tissue characteristics after administration of cardiotoxic chemotherapies using T1-weighted and T2-weighted cardiovascular magnetic resonance. Circ Cardiovasc Imaging 2014;7:872–9.

38. Nakano S, Takahashi M, Kimura F, et al. Cardiac magnetic resonance-based myocardial strain study for evaluation of cardiotoxicity in breast cancer patients treated with trastuzumab: a pilot study to evaluate the feasibility of the method. Cardiol J 2016;23:270–80.

39. Fallah-Rad N, Walker JR, Wassef A, et al. The utility of cardiac biomarkers, tissue velocity and strain imaging, and cardiac magnetic resonance in predicting early left ventricular dysfunction in patients with human epidermal growth factor receptor II-positive breast cancer treated with adjuvant trastuzumab therapy. J Am Coll Cardiol 2011;57:2263–70.

40. Lunning MA, Kutty S, Rome ET, et al. Cardiac magnetic resonance for the assessment of the myocardium after doxorubicin-based chemotherapy. Am J Clin Oncol 2015;38:377–81.

41. Neilan TG, Coelho-Filho OR, Pena-Herrera D, et al. Left ventricular mass in patients with a cardiomyopathy after treatment with anthracyclines. Am J Cardiol 2012;110:1679–86.

42. Lawley C, Wainwright C, Segelov E, Lynch J, Beith J, McCrohon J. Pilot study evaluating the role of cardiac magnetic resonance in monitoring adjuvant trastuzumab therapy for breast cancer. Asia Pac J Clin Oncol 2012;8:95–100.

43. Harries I, Biglino G, Baritussio A, et al. Long term cardiovascular magnetic resonance phenotyping of anthracycline cardiomyopathy. Int J Cardiol 2019;292:248–52.

44. Messroghli DR, Moon JC, Ferreira VM, et al. Clinical recommendations for cardiovascular magnetic resonance mapping of T1, T2, T2* and extracellular volume: a consensus statement by the Society for Cardiovascular Magnetic Resonance (SCMR) endorsed by the European Association for Cardiovascular Imaging (EACVI). J Cardiovasc Magn Reson 2017;19:75.

45. Miller CA, Naish JH, Bishop P, et al. Comprehensive validation of cardiovascular magnetic resonance techniques for the assessment of myocardial extracellular volume. Circ Cardiovasc Imaging 2013;6:373–83.

46. Nakamori S, Dohi K, Ishida M, et al. Native T1 mapping and extracellular volume mapping for the assessment of diffuse myocardial fibrosis in dilated cardiomyopathy. J Am Coll Cardiol Img 2018;11:48–59.

47. Neilan TG, Coelho-Filho OR, Shah RV, et al. Myocardial extracellular volume by cardiac magnetic resonance in patients treated with anthracycline-based chemotherapy. Am J Cardiol 2013;111:717–22.

48. Jordan JH, Vasu S, Morgan TM, et al. Anthracycline-associated T1 mapping characteristics are elevated independent of the presence of cardiovascular comorbidities in cancer survivors. Circ Cardiovasc Imaging 2016;9:e004325.

49. Altaha MA, Nolan M, Marwick TH, et al. Can quantitative CMR tissue characterization adequately identify cardiotoxicity during chemotherapy?: impact of temporal and observer variability. J Am Coll Cardiol Img 2020;13:951–62.

50. Nayak KS, Nielsen JF, Bernstein MA, et al. Cardiovascular magnetic resonance phase contrast imaging. J Cardiovasc Magn Reson 2015;17:71.

51. Chaosuwannakit N, D'Agostino R, Hamilton CA, et al. Aortic stiffness increases upon receipt of anthracycline chemotherapy. J Clin Oncol 2010;28:166–72.

52. Felker GM, Thompson RE, Hare JM, et al. Underlying causes and long-term survival in patients with initially unexplained cardiomyopathy. N Engl J Med 2000;342:1077–84.

53. Meléndez GC, Sukpraphrute B, D'Agostino RB, et al. Frequency of left ventricular end-diastolic volume-mediated declines in ejection fraction in patients receiving potentially cardiotoxic cancer treatment. Am J Cardiol 2017;119:1637–42.

54. Jordan JH, Todd RM, Vasu S, Hundley WG. Cardiovascular magnetic resonance in the oncology patient. J Am Coll Cardiol Img 2018;1:1150–72.

55. Armstrong GT, Plana JC, Zhang N, et al. Screening adult survivors of childhood cancer for cardiomyopathy: comparison of echocardiography and cardiac magnetic resonance. J Clin Oncol 2012;30:2876–84.

56. Zamorano J. An ESC position paper on cardio-oncology. Eur Heart J 2016;37:2739–40.

57. Ganatra S, Carver JR, Hayek SS, et al. Chimeric antigen receptor T-cell therapy for cancer and heart: JACC Council Perspectives. J Am Coll Cardiol 2019;74:3153–63.

58. Kochenderfer JN, Somerville RPT, Lu T, et al. Lymphoma remissions caused by anti-CD19 chimeric antigen receptor T Cells are associated with high serum interleukin-15 levels. J Clin Oncol 2017;35:1803–13.

59. Burstein DS, Maude S, Grupp S, Griffis H, Rossano J, Lin K. Cardiac profile of chimeric antigen receptor T cell therapy in children: a single-institution experience. Biol Blood Marrow Transplant 2018;2:1590–5.

60. Ghosh A, Chen D, Guha A, Mackenzie S, Walker JM, Claire R. CAR T cell therapy-related cardiovascular outcomes and management: systemic disease or direct cardiotoxicity? J Am Coll Cardiol CardioOnc 2020;2:97–109.

61. Ylänen K, Poutanen T, Savikurki-Heikkilä P, Rinta-Kiikka I, Eerola A, Vettenranta K. Cardiac magnetic resonance in the evaluation of the late effects of anthracyclines among long-term survivors of childhood cancer. J Am Coll Cardiol 2013; 61:1539–47.

62. Ylänen K, Eerola A, Vettenranta K, Poutanen T. Three-dimensional echocardiography and cardiac magnetic resonance in the screening of long-term survivors of childhood cancer after cardiotoxic therapy. Am J Cardiol 2014;113:1886–92.

63. Chamsi-Pasha MA, Zhan Y, Debs D, Shah DJ. CMR in the evaluation of diastolic dysfunction and phenotyping of HFpEF: current role and future perspectives. J Am Coll Cardiol Img 2020;13 1 Pt 2: 283–96.

64. Saiki H, Petersen IA, Scott CG, et al. Risk of heart failure with preserved ejection fraction in older women after contemporary radiotherapy for breast cancer. Circulation 2017;135:1388–96.

65. Ferreira de Souza T, Quinaglia A C Silva T, Osorio Costa F, et al. Anthracycline therapy is associated with cardiomyocyte atrophy and preclinical manifestations of heart disease. J Am Coll Cardiol Img 2018;11:1045–55.

66. Mahmood SS, Fradley MG, Cohen JV, et al. Myocarditis in patients treated with immune checkpoint inhibitors. J Am Coll Cardiol 2018;71: 1755–64.

67. Puzanov I, Diab A, Abdallah K, et al. Managing toxicities associated with immune checkpoint inhibitors: consensus recommendations from the Society for Immunotherapy of Cancer (SITC) Toxicity Management Working Group. J Immunother Cancer 2017;5:95.

68. Haanen JBAG, Carbonnel F, Robert C, et al. Management of toxicities from immunotherapy: ESMO Clinical Practice Guidelines for diagnosis, treatment and follow-up. Ann Oncol 2018;29 suppl 4:iv264–6.

69. Bonaca MP, Olenchock BA, Salem JE, et al. Myocarditis in the setting of cancer therapeutics: proposed case definitions for emerging clinical syndromes in cardio-oncology. Circulation 2019; 140:80–91.

70. Zhang L, Awadalla M, Mahmood SS, et al. Cardiovascular magnetic resonance in immune checkpoint inhibitor-associated myocarditis. Eur Heart J 2020;41:1733–43.

71. Ganatra S, Neilan TG. Immune checkpoint inhibitor-associated myocarditis. Oncologist 2018; 23:879–86.

72. Ederhy S, Cautela J, Ancedy Y, Escudier M, Thuny F, Cohen A. Takotsubo-like syndrome in cancer patients treated with immune checkpoint inhibitors. J Am Coll Cardiol Img 2018;11:1187–90.

73. Cammann VL, Sarcon A, Ding KJ, et al. Clinical features and outcomes of patients with malignancy and takotsubo syndrome: observations from the International Takotsubo Registry. J Am Heart Assoc 2019;8:e010881.

74. Eitel I, von Knobelsdorff-Brenkenhoff F, Bernhardt P, et al. Clinical characteristics and cardiovascular magnetic resonance findings in stress (takotsubo) cardiomyopathy. JAMA 2011; 306:277–86.

75. Montalescot G, Sechtem U, Achenbach S, et al. 2013 ESC guidelines on the management of stable coronary artery disease: the task force on the management of stable coronary artery disease of the European Society of Cardiology. Eur Heart J 2013;34:2949–3003.

76. Ibanez B, James S, Agewall S, et al. 2017 ESC Guidelines for the management of acute myocardial infarction in patients presenting with ST-segment elevation: the task force for the management of acute myocardial infarction in patients presenting with ST-segment elevation of the European Society of Cardiology (ESC). Eur Heart J 2018;39:119–77.

77. Dastidar AG, Rodrigues JC, Baritussio A, Bucciarelli-Ducci C. MRI in the assessment of ischaemic heart disease. Heart 2016;102:239–52.

78. Nagel E, Greenwood JP, McCann GP, et al. Magnetic resonance perfusion or fractional flow reserve in coronary disease. N Engl J Med 2019; 380:2418–28.

79. Kristensen SD, Knuuti J, Saraste A, et al. 2014 ESC/ESA Guidelines on non-cardiac surgery: cardiovascular assessment and management [in Polish]. Kardiol Pol 2014;72:857–918.

80. van Nimwegen FA, Schaapveld M, Janus CP, et al. Cardiovascular disease after Hodgkin lymphoma treatment: 40-year disease risk. JAMA Intern Med 2015;175:1007–17.

81. Darby SC, Ewertz M, McGale P, et al. Risk of ischemic heart disease in women after radiotherapy for breast cancer. N Engl J Med 2013;368: 987–98.

82. Correa CR, Litt HI, Hwang WT, Ferrari VA, Solin LJ, Harris EE. Coronary artery findings after left-sided compared with right-sided radiation treatment for early-stage breast cancer. J Clin Oncol 2007;25:3031–7.

83. Machann W, Beer M, Breunig M, et al. Cardiac magnetic resonance findings in 20-year survivors of mediastinal radiotherapy for Hodgkin's disease. Int J Radiat Oncol Biol Phys 2011;79:1117–23.

84. Tichelli A, Bucher C, Rovó A, et al. Premature cardiovascular disease after allogeneic hematopoietic stem-cell transplantation. Blood 2007;11: 3463–71.

85. Lancellotti P, Nkomo VT, Badano LP, et al. Expert consensus for multi-modality imaging evaluation of cardiovascular complications of radiotherapy in adults: a report from the European Association of Cardiovascular Imaging and the American Society of Echocardiography. Eur Heart J Cardiovasc Imaging 2013;14:721–40.

86. Hull MC, Morris CG, Pepine CJ, Mendenhall NP, et al. Valvular dysfunction and carotid, subclavian, and coronary artery disease in survivors of Hodgkin lymphoma treated with radiation therapy. JAMA 2003;290:2831–7.

87. Maraldo MV, Ng AK. Minimizing cardiac risks with contemporary radiation therapy for Hodgkin lymphoma. J Clin Oncol 2016;34:208–10.

88. Caruthers SD, Lin SJ, Brown P, et al. Practical value of cardiac magnetic resonance for clinical quantification of aortic valve stenosis: comparison with echocardiography. Circulation 2003;108: 2236–43.

89. Søndergaard L, Hildebrandt P, Lindvig K, et al. Valve area and cardiac output in aortic stenosis: quantification by magnetic resonance velocity mapping. Am Heart J 1993;126:1156–64.

90. Piccirillo JF, Tierney RM, Costas I, Grove L, Spitznagel EL. Prognostic importance of comorbidity in a hospital-based cancer registry. JAMA 2004;291:2441–7.

91. Wu S, Chen JJ, Kudelka A, Lu J, Zhu X. Incidence and risk of hypertension with sorafenib in patients with cancer: a systematic review and meta-analysis. Lancet Oncol 2008;9:117–23.

92. Maceira AM, Mohiaddin RH. Cardiovascular magnetic resonance in systemic hypertension. J Cardiovasc Magn Reson 2012;14:28.

93. Valent P, Hadzijusufovic E, Schernthaner GH, Wolf D, Rea D, le Coutre P. Vascular safety issues in CML patients treated with BCR/ABL1 kinase inhibitors. Blood 2015;125:901–6.

94. Fajardo LF. Is the pathology of radiation injury different in small vs large blood vessels? Cardiovasc Radiat Med 1999;1:108–10.

95. Plana JC, Galderisi M, Barac A, et al. Expert consensus for multimodality imaging evaluation of adult patients during and after cancer therapy: a report from the American Society of Echocardiography and the European Association of Cardiovascular Imaging. J Am Soc Echocardiogr 2014;27:911–39.

96. Rhodes M, Lautz T, Kavanaugh-Mchugh A, et al. Pericardial effusion and cardiac tamponade in pediatric stem cell transplant recipients. Bone Marrow Transplant 2005;36:139–44.

97. Bogaert J, Francone M. Cardiovascular magnetic resonance in pericardial diseases. J Cardiovasc Magn Reson 2009;11:14.

98. Kramer CM, Barkhausen J, Flamm SD, Kim RJ, Nagel E. Standardized cardiovascular magnetic resonance (CMR) protocols 2013 update. J Cardiovasc Magn Reson 2013;15:91.

99. Hoey ET, Gulati GS, Ganeshan A, Watkin RW, Simpson H, Sharma S. Cardiovascular MRI for assessment of infectious and inflammatory conditions of the heart. AJR Am J Roentgenol 2011; 197:103–12.

100. Taunk NK, Haffty BG, Kostis JB, Goyal S. Radiation-induced heart disease: pathologic abnormalities and putative mechanisms. Front Oncol 2015;5:39.

101. Flett AS, Hayward MP, Ashworth MT, et al. Equilibrium contrast cardiovascular magnetic resonance for the measurement of diffuse myocardial fibrosis: preliminary validation in humans. Circulation 2010;122:138–44.

102. Karamitsos TD, Piechnik SK, Banypersad SM, et al. Noncontrast T1 mapping for the diagnosis of cardiac amyloidosis. J Am Coll Cardiol Img 2013;6:488–97.

103. Banypersad SM, Sado DM, Flett AS, et al. Quantification of myocardial extracellular volume fraction in systemic AL amyloidosis: an equilibrium contrast cardiovascular magnetic resonance study. Circ Cardiovasc Imaging 2013;6:34–9.

104. Maceira AM, Joshi J, Prasad SK, et al. Cardiovascular magnetic resonance in cardiac amyloidosis. Circulation 2005;111:186–93.

105. Falk RH, Quarta CC, Dorbala S. How to image cardiac amyloidosis. Circ Cardiovasc Imaging 2014;7:552–62.

106. Armenian SH, Lacchetti C, Barac A, et al. Prevention and monitoring of cardiac dysfunction in survivors of adult cancers: American Society of Clinical Oncology Clinical Practice Guideline. J Clin Oncol 2017;35:893–911.

107. Vermersch M, Longere B, Coisne A, et al. Compressed sensing real-time cine imaging for assessment of ventricular function, volumes and mass in clinical practice. Eur Radiol 2020;30:609–19.

108. Ferrari VA, Whitman B, Blankenship JC, et al. Cardiovascular imaging payment and reimbursement systems: understanding the past and present in order to guide the future. J Am Coll Cardiol Img 2014;7:324–32.

109. Garg R, Sevilla A, Garberich R, Fleishman CE. Remote delivery of congenital cardiac cardiac magnetic resonance services: a unique telemedicine model. Pediatr Cardiol 2015;36:226–32.

110. Cardinale D, Colombo A, Bacchiani G, et al. Early detection of anthracycline cardiotoxicity and improvement with heart failure therapy. Circulation 2015;131:1981–8.

111. Yeh ET, Bickford CL. Cardiovascular complications of cancer therapy: incidence, pathogenesis, diagnosis, and management. J Am Coll Cardiol 2009;53:2231–47.

112. Khakoo AY, Kassiotis CM, Tannir N, et al. Heart failure associated with sunitinib malate: a multitargeted receptor tyrosine kinase inhibitor. Cancer 2008;112:2500–8.

113. Cornell RF, Ky B, Weiss BM, et al. Prospective study of cardiac events during proteasome inhibitor therapy for relapsed multiple myeloma. J Clin Oncol 2019;37:1946–55.

114. Barthur A, rezden-Masley C, Connelly KA, et al. Longitudinal assessment of right ventricular structure and function by cardiovascular magnetic resonance in breast cancer patients treated with trastuzumab: a prospective observational study. J Cardiovasc Magn Reson 2017;19:44.

115. Nazarian S, Hansford R, Rahsepar AA, et al. Safety of cardiac magnetic resonance in patients with cardiac devices. N Engl J Med 2017;377:2555–64.

116. Marano AA, Henderson PW, Prince MR, Dashnaw SM, Rohde CH. Effect of MRI on breast tissue expanders and recommendations for safe use. J Plast Reconstr Aesthet Surg 2017;70:1702–7.

117. Woolen SA, Shankar PR, Gagnier JJ, MacEachern MP, Singer L, Davenport MS. Risk of nephrogenic systemic fibrosis in patients with stage 4 or 5 chronic kidney disease receiving a group ii gadolinium-based contrast agent: a systematic review and meta-analysis. JAMA Intern Med 2019;180:223–30.

KEY WORDS cardio-oncology, cardiotoxicity, cardiovascular magnetic resonance, chemotherapy, left ventricular dysfunction, tissue characterization

Go to http://www.acc.org/jacc-journals-cme to take the CME/MOC/ECME quiz for this article.